



**MODELLING THE RESPONSE OF CYTOTOXIC  
T-LYMPHOCYTES IN CONTROLLING SOLID  
TUMOUR INVASION**

A DISSERTATION SUBMITTED TO THE UNIVERSITY OF KwaZULU-NATAL  
FOR THE DEGREE OF MASTER OF SCIENCE  
IN THE COLLEGE OF AGRICULTURE, ENGINEERING & SCIENCE

By

**JOSEPH MALINZI**

School of Mathematics, Statistics & Computer Science

June 2013

# Abstract

We present mathematical models to study the mechanism of interaction of tumour infiltrating cytotoxic lymphocytes (TICLs) with tumour cells. We focus on the phase spaces of the systems and the nature of the solutions for the cell densities in the short and long term. The first model describes the production of offspring through cell proliferation, death and local kinetic interactions. The second model characterises the spatial distribution dynamics of the cell densities through reaction diffusion, which describes the random movement of the cells, and chemotaxis, which describes the immune cell movements towards the tumour cells. We then extend these models further to incorporate the effects of immunotherapy by developing two new models. In both situations, we analyse the phase spaces of the homogeneous models, investigate the presence of travelling wave solutions in our systems, and provide numerical simulations. Our analysis shows that cancer dormancy can be attributed to TICLs. Our study also shows that TICLs reduce the tumour cell density to a cancer dormant state but even with immunotherapy do not completely eliminate tumour cells from body tissue. Travelling wave solutions were confirmed to exist in the heterogeneous model, a linear stability analysis of the homogeneous models and numerical simulations show the existence of a stable tumour dormant state and a phase space analysis confirms that there are no limit cycles.



# Acknowledgements

It is not by chance that I am alive, and so to God be the glory. I thank my mum and dad for generously believing in me even when I did not. I am grateful to my supervisors Prof. P. Sibanda and Dr. H. Mambili-Mamboundou for their guidance and support. I also acknowledge the contribution of the African Institute for Mathematical Sciences and the School of Mathematics Statistics and Computer Science, UKZN for their financial support.

I dedicate this dissertation to my mum.

# Contents

<b>Abstract</b>	<b>i</b>
<b>Declaration</b>	<b>ii</b>
<b>Acknowledgements</b>	<b>iii</b>
<b>List of Figures</b>	<b>viii</b>
<b>List of Tables</b>	<b>ix</b>
<b>1 Introduction</b>	<b>1</b>
1.1 Motivation and aim of the study . . . . .	1
1.2 Cancer . . . . .	3
1.2.1 Cancer in general . . . . .	3
1.2.2 Immune system response to cancer and treatments . . . . .	5
1.3 Review of cancer modelling studies . . . . .	7
1.3.1 Tumour growth models . . . . .	7
1.3.2 Classification of avascular tumour growth models . . . . .	9
1.3.3 Fisher-Kolmogorov equation . . . . .	11

1.3.4	Keiller-Seigel model . . . . .	11
1.3.5	Receptor-ligand kinetics . . . . .	12
1.3.6	Tumour-cytotoxic T-lymphocyte interactions . . . . .	13
1.3.7	Results from prior modelling studies . . . . .	14
1.4	Methodology used . . . . .	15
1.4.1	Benchmark modelling criteria . . . . .	15
1.4.2	Congruent assumptions . . . . .	16
1.4.3	Models used . . . . .	17
1.5	Overview . . . . .	20
<b>2</b>	<b>Local kinetic interactions</b>	<b>21</b>
2.1	Model formulation . . . . .	21
2.2	Boundedness and feasibility analysis . . . . .	26
2.3	Steady state solutions and stability analysis . . . . .	29
2.3.1	Threshold condition . . . . .	31
2.3.2	Investigating global stability of the TFE . . . . .	32
2.4	Sensitivity and phase space analysis . . . . .	34
2.5	Numerical simulations . . . . .	38
<b>3</b>	<b>Spatially heterogeneous model</b>	<b>43</b>
3.1	Introduction . . . . .	43
3.2	Boundary and initial conditions . . . . .	48
3.3	Parameters estimation . . . . .	48

3.4	Non-dimensionalization of equations . . . . .	49
3.5	Numerical simulations . . . . .	51
3.5.1	Methodology . . . . .	52
3.5.2	Numerical simulation results . . . . .	55
3.6	Travelling wave simulation and analysis . . . . .	56
<b>4</b>	<b>TICLs-tumour cell interaction with immunotherapy</b>	<b>62</b>
4.1	Model development . . . . .	63
4.2	Non-dimensionalization . . . . .	66
4.3	Steady state solutions and stability analysis . . . . .	67
4.4	Phase space analysis . . . . .	68
4.5	Numerical simulations of the model . . . . .	71
4.6	Immunotherapy model in a spatially heterogeneous domain . . . . .	73
4.6.1	Model development . . . . .	73
4.6.2	Numerical solutions . . . . .	77
<b>5</b>	<b>Conclusion</b>	<b>80</b>
	<b>Appendices</b>	<b>83</b>
	<b>References</b>	<b>86</b>

# List of Figures

1.1	Schematic diagram showing the three layer structure of a tumour.	4
2.1	A diagram showing local interactions between T-cells and tumour cells, cells' proliferation and death. . . . .	23
2.2	Diagram showing the direction vector field on $D_1$ and $D_2$ . . . . .	28
2.3	Phase space of the ODE system (2.5). The phase plane is a stable focus converging to the tumour dormant state. . . . .	36
2.4	Phase plots showing the direction fields corresponding to parameter values (a) $\sigma_1 = 0.001$ , (b) $\sigma_1 = 1$ , (c) $\mu = 0.3$ and (d) $\mu = 3$ respectively. . . . .	37
2.5	Plots of cell densities against non-dimensional time. . . . .	39
2.6	Plots of immune (TICLs) and tumour cell densities against non-dimensional time time on different scales. . . . .	39
2.7	Contour plots showing the effect of the parameters $\sigma_1$ , $\beta_1$ and $\mu$ as (a) $\sigma_1$ and $\mu$ change, with $\beta_1$ fixed. (b) $\beta_1$ and $\mu$ change, with $\sigma_1$ fixed. . . . .	42
3.1	Initial cell densities of TICLs and tumour cells. . . . .	51

3.2	Spatial distribution of immune (TICLs) and tumour cell densities in the tissue at times corresponding to (a) 600, (b) 700, (c) 800 and (d) 1000 days respectively. The left and right hand scales correspond to TICLs and tumour cell densities respectively. . . . .	55
3.3	Travelling wave solutions of the system (3.18) for a long (a,b) and short time periods (c,d). . . . .	57
4.1	Orbit of the ODE system (4.2) converging to the tumour dormant state. . . . .	70
4.2	Plots of cell densities with immunotherapy against non-dimensional time. . . . .	72
4.3	Variation of immune (TICLs) and tumour cell densities with immunotherapy against time. The time is non-dimensional . . . . .	73
4.4	Plots of solutions showing spatial distribution of immune (TICLs) and tumour cell densities with immunotherapy in the tissue at times corresponding to (a) 600, (b) 700, (c) 800 and (d) 1000 days respectively. The left and right hand scales correspond to TICLs and tumour cell densities respectively. . . . .	78

# List of Tables

2.1	State variables for the tumour-immune cells model (2.1). . . . .	24
2.2	Parameter description for the tumour-immune cells interaction model (2.1). . . . .	24
2.3	Dimensional parameter values obtained from Matzavinos et al. [6].	38
3.1	Parameter values for diffusion and chemotaxis. . . . .	49
4.1	State variables for the tumour-immune cells model with immunotherapy (4.1). . . . .	64
4.2	Newly introduced Parameter description for the tumour-immune cells interaction model with immunotherapy (4.1). . . . .	65
4.3	Dimensional parameter values obtained from Kirschener and Panetta [32] and Borges et al. [66]. . . . .	69

# Chapter 1

## Introduction

### 1.1 Motivation and aim of the study

The origin of the term cancer is ascribed to Hippocrates (460-370BC). He used the terms *carcinos* and *carcinoma* to describe non-ulcer and ulcer-forming tumours. Later, Celsus (28-50BC) translated these terms into cancer [1]. Cancer, known medically as a malignant neoplasm is a group of diseases, all involving un-regulated cell growth. Tumours can be benign or malignant (cancerous). Cancer cells divide irrepressibly forming cancerous tumours, and can invade adjacent parts of the body. There are several types of tumours with names usually reflecting either the kind of tissue in which they arise in, or suggestive of the shape or manner of tumour growth. For example, meningioma is a tumour that arises from meninges, the system of membranes that cover the central nervous system. Diagnosis depends on the type and location of the tumour [2].

Organs in the body are made up of cells. These cells replicate as the body needs them. If the cells continue multiplying irrepressibly, a mass of tissue known as a tumour may be formed [3]. These growths are either benign (non cancerous) or

malignant (cancerous). Benign tumours do not spread to other parts of the body and are often easily removed whereas malignant tumours invade nearby tissues and spread to other parts of the body. Cancer can result from chemical exposure, cells skipping certain phase transitions, chronic infections, medicinal drugs, immunosuppression, and gene mutations [2]. Yashiro et al. [4] state that cell evolutionary processes may give rise to an abnormal DNA thus causing cancer. For instance he stresses that more than four-fifths of colorectal cancer evolve as a consequence of chromosomal instability. A proper and definitive cure to several cancers does not yet exist despite modern cancer therapies such as radiotherapy, medical oncology, and chemotherapy. However, the World Health Organisation in the 2012 *cancer report* [5] states that cancers are preventable and the primary goal of prevention is to stop the growth of cancerous cells by reducing exposure to cancer causing factors such as environmental carcinogens or lifestyle factors such as poor nutrition. According to the World Health Organisation [5], 7.6 million people worldwide died from cancer in 2008. Approximately 70% of cancer deaths occur in low and middle-income countries. The same report, however, indicates that 30% of the cancers could have been prevented. The report also indicates that cancer is the second major killer cause of deaths in Europe responsible for 25% of total deaths after cardiovascular diseases.

Despite various control measures that have been implemented, cancer is still a leading cause of death in the world [2]. Much is still not known about the dynamics of its growth and destructive strategies. Further more, little is known about cancer dormancy, limiting the comprehension of the full complexity and dynamics of the disease [6]. Cancer is therefore of major public health interest. For this, and other socio-economic related reasons, much effort is needed to understand the dynamics of tumour-immune interactions.

Our aim therefore, is to use mathematical models to understand the interaction between tumour cells and cytotoxic infiltrating T-lymphocytes and investigate the phenomenon of cancer dormancy as a result of these interactions. Later we incorporate immunotherapy to determine the effect it has on both immune and tumour cell densities in the human body. Efforts in this line have been made before by Matzavinos et al. [6] and Zeyton et al. [7]. Understanding this interaction could help in predicting the impact of immunotherapy on cancer and possibly help plan control strategies or develop more efficient and effective anti cancer drugs.

## 1.2 Cancer

In this section, we briefly explain cancer, discuss the major steps in cancer progression, and highlight immunotherapy, a form of intervention.

### 1.2.1 Cancer in general

Tumours are known to progress through two or three distinct growth stages; the avascular and vascular growth stages. The avascular stage is the earliest stage during which cells begin to replicate uncontrollably. During the vascular stage, proliferating tumour cells move into the blood stream thus spreading to other parts of the body [8]. The vascular stage consists of two phases, the angiogenetic phase, during which tumour cells secrete tumour angiogenetic factors (TAF), which attract blood vessels toward the tumour, by forming secondary blood vessels that provide the tumour with unlimited nutrients. The last phase is metastasis, where tumour cells migrate to the blood stream and invade other parts of the body. The tumour nodule is made up of three layers, the necrotic core, quiescent layer, and proliferating zone. The necrotic core at the centre forms when cells are deprived

of vital nutrients and end up dying. The proliferating cells are in the outer layers. In between these regions, lie the nascent cells which form the quiescent layer. Chaplain et al. [9] states that a fraction of these can be recruited into the layer of proliferating cells. These three layer structures are shown schematically in Figure 1.1.

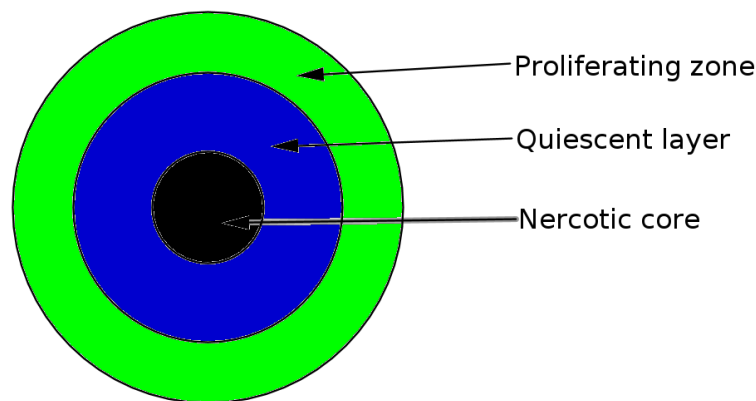


Figure 1.1: **Schematic diagram showing the three layer structure of a tumour.**

In the development of a tumour from the avascular to the vascular stage, within the tumour bears the ability to invade surrounding tissue and metastasise to distant parts of the body. This depends upon its ability to induce new blood vessels from surrounding tissue to sprout towards the tumour which gradually penetrate it, thus providing the tumour with an adequate blood supply and microcirculation [9]. However, tumour growth may not systematically go through all the three stages. There is clinical evidence that some people live with benign tumours for their entire life time [10]. This pause can be explained by cancer dormancy, a situation where the tumour cells are neither proliferating nor dying. Cancer dormancy is however poorly understood [6]. Recent studies, for

example Matzavinos et al. [6] have established that cancer dormancy could be caused by tumour infiltrating cytotoxic lymphocytes (TICLs). When an immune cell comes into contact with a tumour cell, it sends a signal to other immune cells by secreting a chemical (chemokine). These immune cells react to the signal by chemotactically moving towards the tumour nodule [6]. The phenomenon where somatic cells, bacteria and other single-cell or multi cellular organisms move in accordance with an external chemical stimulus spread in the environment is known as chemotaxis [11]. The immune cells are either tumour infiltrating cytotoxic-lymphocytes (TICLs), meant to directly contact infected cells or others that do not necessarily attack infected cells for example phagocytes. The TICLs may be cytotoxic lymphocytes (CTLs, CD8<sup>+</sup> cells), natural killer-like cells (NK) and/or lymphokine activated killer cells (LAK) [6, 12]. This family of T-cells is believed to keep the tumour cells at a dormant level and for longer time periods.

### **1.2.2 Immune system response to cancer and treatments**

MD Coley, a New York surgeon first noted in the 1800's that contracting an infection seemed to help some cancer patients. He began treating cancer patients by deliberately infecting them with certain bacteria, which became known as Coley toxins. His techniques have since been superseded by other types of cancer treatment as doctors have learnt more about the immune system. In modern treatments, two basic conditions should be fulfilled in order for a cancer treatment to be considered effective. It should firstly destroy the cancer cells and should also distinguish between cancerous and healthy cells [12]. It is possible to do this through immunotherapy. The role of the immune system in tumour eradication has been clearly established [13]. However, the biological knowledge required to win the battle against cancer is still limited just as stated by Lollini et al. [13]. The

earliest evidence of anti-tumour immune reactivity was witnessed in the 1940's and 1950's by showing that inbred mice vaccinated against syngeneic tumours had a good immune memory although they had less immune specificity required to target specific antigens, Lollini et al. [13]. This type of finding led to the establishment of the "immune surveillance" theory. The theory postulated that the protection of the host from carcinogenesis and tumour development was a cardinal function of the immune system [14]. The way in which the immune cells fight tumour cells is summarised by Lollini et al. [13] as follows.

Phagocytic cells such as macrophages and granulocytes have a two fold role in immunity against tumours. They directly attack and destroy the tumour cells and at the same time generate cell degradation products that are picked up by antigen presenting cells (APCs). Dendritic cells (DCs) are the APCs that pick up those tumour antigens in the boundaries, then move to the lymph nodes so as to present them to the TILs. This process in which antigens are presented and cytokines released, is an indispensable and essential action for the initiation of all primary immune systems. After antigen presentation, helper cells proliferate and secrete cytokines to activate TILs that in turn kill the tumour cells. B-cells play a minimal role in immune responses to solid tumours. As can be seen, TILs play a major role in tumour eradication. This was in essence deduced from experimental results and clinical approaches done by Rosenberg et al. [15].

Immunotherapy falls into three major categories. Firstly, it can enhance the natural immune response, or secondly, specific antibodies are introduced, or thirdly, vaccines are used. The first category involves using substances that boost the immune system such as interleukines. For example interleukine-2 (IL2) [16]. In the second category, Monoclonal antibodies are formulated to target specific cancer antigens. These antibodies can distinguish between normal and cancer cells and

so they can be used both to diagnose cancer and to treat tumours by directing anti cancer drugs towards malignant cells [17, 18]. The third category involves therapeutic use of vaccines. These vaccines being specifically created to target tumour cells. Among many examples of such vaccines, there are Cell genesys (GVAX), Cancer vax (canvaxin), and Genitop Corp. In this dissertation, we shall consider only the first category of immunotherapy, that protein like substances, specifically IL2 are injected into a human body to stimulate the immune system thus boosting the immune response.

## **1.3 Review of cancer modelling studies**

Research on cancer greatly advanced in the nineteenth century when Rudolf Virchow who is often referred to as the father of cellular pathology, provided the scientific basis for the modern study of cancer [1]. Mathematical modelling also began around the same time with a logistic growth equation being used to describe tumour growth (see [19]). In this section, we present some famous tumour growth models and classify models that have been previously used to model tumour growth at the avascular stage. We then, briefly discuss some major phenomena used in this dissertation (diffusion and chemotaxis). Finally, we present the Matzavinos et al. [6] model. A model that we rely on in this dissertation to construct our models.

### **1.3.1 Tumour growth models**

We begin with a brief review of the three basic growth models used for describing tumour growth, namely the exponential growth model, the Compertz growth model, and models based on metabolic considerations.

1. **Exponential growth model** This model assumes that all tumours follow a standard pattern of growth, growing fastest at the beginning of a time period and eventually reaching a plateau [19]. The major shortfall of this model is that it is unable to model the behaviour in vivo.
2. **Gompertz growth model** The Gompertz curve or function, developed by Benjamin Gompertz, is a mathematical model for a time series, where growth slows down at the end of a time period [19]. It was however suggested that this function is unable to sufficiently model clinical data because tumour cells almost certainly have different growth characteristics in different patients, and individual micrometastases within a single patient may also have different growth parameters (see [19]). In the 1960s, Laird [20] was the first to successfully use the Gompertz logistic growth function to fit data to the growth of tumours. Another setback of this model is that different individuals have got different parameters.
3. **Model based on metabolic considerations** This model is at times referred to as the universal law. It describes the chemical transformations within the tumour cells. The major disadvantage associated with the universal law model is that there are so many parameters to determine and each individual or organism would require a different set of parameters which is not feasible (see [19]).

The mathematical models describing tumour-immune interaction are usually ordinary differential equations (ODEs), delay differential equations (DDEs) or partial differential equations (PDEs) depending on the physical aspects considered. These models could be stochastic or through a deterministic regime like Kolmogorov-Petrovsky-Piskounov-Fisher (KPP-Fisher) model [21].

### 1.3.2 Classification of avascular tumour growth models

It is not easy to describe all tumour growth models. However, all avascular tumour growth models can be categorised as either (1) microscopic or (2) macroscopic growth models. Rose et al. [22] further classify avascular tumour models into two basic categories: (1) continuum mathematical models that incorporate space and thus are made up of partial differential equations, and (2) discrete population models that consider dynamics occurring on a single cell scale and incorporate cell to cell interactions.

#### Microscopic tumour growth models

Microscopic models are based on microscopic observations, both in-vivo and in-vitro. They model growth dynamics basing on observations including the acidity of the cells, vascularization or internal cell dynamics [23]. They strive to incorporate physical and chemical interactions between cancer cells, the extra-cellular matrix and healthy cells. Mechanical phenomena such as pressure, cohesion and adhesion forces in the cells are often included in these descriptions. As for chemical interactions, microscopic models incorporate phenomena such as the diffusion of nutrients and oxygen in the cells, secretion of different diffusible factors by tumour cells and their effects on the surrounding [24]. As a consequence, there are many parameters for such models. Specific factors that are normally modelled at a microscopic level include mitosis, cell division, distribution and consumption of oxygen, apoptosis, surface tension, cell cycles, diffusion, and chemotaxis. From a technical point of view, formulations of microscopic models allow for a large variety of mathematical methods. The systems used to characterize microscopic models are PDEs, cellular automata and statistical models. Some studies further

classify microscopic models into avascular, angiogenesis, and vascular growth models, the tumour growth stages. Some examples of microscopic models can be found in [26, 27, 28, 29]. Nevertheless Araujo and McElwain [25] maintain that tumour-immune interactions at a microscopic level is limited.

### **Macroscopic tumour growth models**

Macroscopic models are based on observations on a macroscopic level, for instance, magnetic resonance images (MIR), computed tomography (CT) scans, and diffusion tensor images (MR-DTI) [24]. Because observable factors are not so many, macroscopic models incorporate only a few factors and so are mathematically simpler than microscopic models. Factors normally considered in macroscopic models include cell proliferation and death, diffusion and chemotaxis. Some studies further classify macroscopic models into mechanical and diffusive models. Mechanical models consider the mechanical interactions between tumour cells. They are used with the aim of providing answers to questions pertaining to about how the mechanical properties of the tumour, and the tissue in which the tumour grows, influence growth [22]. Diffusive models concentrate on reaction-diffusion formalism. In this dissertation, we consider a macroscopic scale. Some examples of macroscopic models can be found in [6, 8, 30, 31, 32, 33].

Next, we review some models that have been used to model certain aspects of cancer evolution, immune cell movement and tumour-immune interactions. The models incorporate the diffusion of both tumour and immune cells, chemotaxis (which models immune cell movement), apoptosis for both tumour and immune cells, and local kinetic interactions between the tumour and immune cells.

### 1.3.3 Fisher-Kolmogorov equation

The Fisher-Kolmogorov equation, also known as the Fisher-KPP equation, is the simplest macroscopic reaction-diffusion evolution equation for modelling cancer invasion [33]. It has been used frequently in modelling diffusive tumours and the evolution of cancer on a macroscopic scale [33, 34, 35]. The system

$$\frac{\partial C}{\partial t} = \nabla \cdot (D(x) \nabla C) + \rho C(1 - C), \quad (1.1a)$$

$$D \cdot \nabla \vec{n}_{\partial\Omega} = 0, \quad (1.1b)$$

is the basic building block of such reaction diffusion models where  $C$  is the tumour cell density,  $D$  is the diffusivity,  $\rho$  is the proliferation rate of the tumour cells,  $\Omega$  is the domain under consideration and  $\partial\Omega$  represents the boundaries of the tumour tissue. Equation (1.1a) describes the evolution of the tumour cell density distribution whereas (1.1b) represents the no-flux boundary conditions [33].

### 1.3.4 Keiller-Seigel model

The Patlak/Keller-Seigel model considers the density  $n(x, t)$  of cells and the chemoattractant density  $C(x, t)$  assuming that the cells emit the chemoattractant directly which is then instantly diffused [11]. The Keiler-Seigel chemotaxis model has the form

$$\frac{\partial n}{\partial t} = \Delta n - \chi \nabla \cdot (n \nabla C), \quad t > 0, x \in \mathbb{R}^d, \quad (1.2a)$$

$$-\Delta C = n, t > 0, \quad x \in \mathbb{R}^d, \quad (1.2b)$$

$$n(0, x) = n_0(x) \geq 0, \quad x \in \mathbb{R}^d, \quad (1.2c)$$

$\chi$  is the chemotactic sensitivity function,  $C$  is the chemical density and  $n$  is the cell density. Equation (1.2b) describes the Dirichlet boundary conditions and equation (1.2c) describes the initial conditions. Other models however, such as Myerscough et al. [36] use the Neumann boundary conditions, based on the assumption that neither the cells nor the chemo-attractant are able to cross the boundary of the domain. In this study, we make the same assumption and thereby use the Neumann boundary conditions.

### 1.3.5 Receptor-ligand kinetics

Receptor-ligand interactions form the backbone of many biological processes such as signal transduction, physiological regulation, gene transcription, and enzymatic reactions [37]. Kinetics is a generic term used to describe both rates at which processes occur and the field associated with study of rates [38]. A receptor is a biological target that binds specifically with small molecules (ligands) resulting in certain biological responses [39]. For any similar molecules that associate, it is possible to consider one as the a ligand and the other as a receptor [38]. The simplest representation of the receptor-ligand kinetics is through stoichiometry, a term used to refer to how many molecules of ligand can bind to a receptor. Lauffenburger and Linderman [38] used the simple equation to describe the receptor-ligand kinetics.



where  $R$  is the receptor,  $L$  is the ligand and  $RL$  is the receptor-ligand complex formed after the ligand binding to the receptor.  $K_f$  is a parameter describing the forward rate whereas  $k_r$  is the reverse constant rate. Taking this chemical kinetics and applying it to cells, we consider the tumour cells to be the receptors and the tumour infiltrating cytotoxic lymphocytes to be the ligands. The TICLs bind to the tumour cells to form tumour-TICLs complexes [31, 40].

### 1.3.6 Tumour-cytotoxic T-lymphocyte interactions

Matzavinos et al. [6] developed a model for the attack of tumour cells by TICLs without necrosis and at some stage before angiogenesis. This model used reaction diffusion and chemotaxis kinetics. The basic findings of this model include existence of periodic solutions in the phase space, travelling wave solutions, oscillatory kinetics of tumour-immune densities, and evolution of cancer dormancy. Matzavinos et al. [6] considered a tumour density  $T$ , a TICLs density  $E$ , a chemokine concentration secreted by the TICLs  $\alpha$ , tumour-TICLs complex density  $C$ , dead TICLs  $E^*$  and dead tumour cells  $T^*$ . The complete system is

$$\frac{\partial E}{\partial t} = D_1 \nabla^2 E - \chi \nabla \cdot (E \nabla \alpha) + sh(x) + \frac{fC}{g + T} - d_1 E - k_1 ET + (k_{-1} + k_2 p)C, \quad (1.4a)$$

$$\frac{\partial \alpha}{\partial t} = D_2 \nabla^2 \alpha + k_3 C - d_4 \alpha, \quad (1.4b)$$

$$\frac{\partial T}{\partial t} = D_3 \nabla^2 T + b_1(1 - b_2 T)T - k_1 ET + (k_{-1} + k_2(1 - p))C, \quad (1.4c)$$

$$\frac{\partial C}{\partial t} = k_1 ET - (k_{-1} + k_2)C, \quad (1.4d)$$

$$\frac{\partial E^*}{\partial t} = k_2(1 - p)C - d_2 E^*, \quad (1.4e)$$

$$\frac{\partial T^*}{\partial t} = k_2 p C - d_3 T^*, \quad (1.4f)$$

where  $D_1$ ,  $D_2$  and  $D_3$  are diffusion constants for the TICLs, tumour and chemokine concentrations respectively,  $\chi$  is the chemotaxis constant,  $s$  is a parameter representing the supply of immune cells into the tumour localization,  $h(x)$  is a heaviside function to differentiate tumour and immune cells localization,  $fC/(g + T)$  is the proliferation function,  $d_1$ ,  $d_2$ ,  $d_3$ , and  $d_4$  are de-activation rates of the immune cells, de-activated immune cells, lethally hit tumour cells and tumour cells respectively and  $b_1(1 - b_2T)$  is a tumour propagation term. The TICL-tumour complex is dissociated at a rate  $k_1$ ,  $k_2$  is a parameter describing the rate of detachment of TICLs from tumour cells resulting into death of the tumour cells,  $k_{-1}$  is the rate of detachment of TICLs from tumour cells without damaging the cells  $p$  is a parameter representing the probability of tumour death and  $k_3$  is the chemokine production rate.

### 1.3.7 Results from prior modelling studies

We list some previously published results from tumour-immune modelling studies.

- A stable cancer dormant state exists where the immune cells manage to take the tumour cells to a level where they neither proliferate nor die, Matzavinos et al. [6] and Randuskaya et al. [16]. Some modelling studies, for example, Wordaz and Jansen [41] have shown that the cancer dormant state may later cease and there may be a tumour regrowth, thus showing the dormant state to be unstable. However, empirical evidence would suggest that this is not achievable in real life as for such a situation to occur, it would take thousands of years, a life span that is not feasible.

- The immune cells are capable of reducing the level of tumour cell concentration, but do not completely eliminate them from the tissue, Matzavinos et al. [6], Zeyton et al. [7] and Randuskaya et al. [16].
- Oscillatory dynamics of the immune and tumour cell concentrations in the tissue. These oscillations are possibly as a result of diffusion of both cell concentrations in the tissue and the local kinetic interactions, Matzavinos et al. [6].

In this dissertation, we seek to expound on cancer dormancy, a phenomenon attributed to tumour-immune cell interactions. We seek to investigate the dynamics of the tumour and immune cells and also see the effects of treatment, in our case immunotherapy on these interactions.

## 1.4 Methodology used

In this section, we present the assumptions we consider in this dissertation to construct our models, methods, and the aspects that we choose to analyse.

### 1.4.1 Benchmark modelling criteria

It is common understanding that any useful mathematical model should have a minimum number of parameters, the variables should be measurable and the model's predictions should be reasonably accurate so as to give a good fit to experimental data. Ellner and Guckenheimer [42] set out the steps of what one should follow in the process of model construction. According to Chaplain [9], the major questions to consider in cancer-immune modelling are whether modelling is done in vivo or in vitro, the scale of description; whether it is sub cellular,

cellular, or the whole organism is considered, whether space is considered or not, and whether the cell cycle is represented and whether cell invasion is represented. It is impractical to incorporate all natural processes involved in cancer-immune response into a single model. However, Chaplain [9] notes that a realistic model should include certain nonuniformities in the central processes of inhibition of mitosis, namely: the consumption of nutrients, cell proliferation, geometrical constraints and central necrosis. Bru' et al. [44] further stress that the central physical aspects describing macroscopic spatial dynamics of avascular tumours, a scale we consider in this dissertation, are proliferation of cells in the outer rim, cell diffusion along the tumour tissue border surface and the linear growth of tumour radius after a critical time but before exponential growth.

### 1.4.2 Congruent assumptions

In previous tumour-immune models, certain assumptions have been made. They are derived from experimental results, published statements or theories coupled with reasonable suppositions [6, 7, 16, 41, 43, 45, 49]. We list some of the most important adopted in this work.

- Tumour cells progress logistically in the absence of immune response. This growth model was used by Briton [49], and fitted into real data by Diefenbach et al. [43].
- TICLs are capable of killing tumour cells [6, 16, 43, 45].
- Tumour cells interact with TICLs in such a way that tumour-cell complexes are formed. When a TICL binds to a tumour cell, it can lead to either the tumour cell being killed or the TICL being inactivated [6].

- Immune cells are normally present in the body, even when no tumour cells are present, because they are part of the innate immune system [16]. This is a reason for a source term for immune cells being included in our model.
- TICLs have an element of random motility and also respond chemotactically to chemokines, Matzavinos et al. [6].
- Diffusion and chemotaxis is considered to be linear [6]. Although this assumption may be unrealistic, it is necessary for the sake of simplicity.
- The dead immune and tumour cells do not influence the formation of cellular conjugates [6].

In addition to the above assumptions above, we also assume that

- the formation of cellular conjugates occurs in a time frame of several minutes to a few hours whereas that of tumour cells as well as the influx of immune cells into the spleen occurs on a much slower time scale. This is the same assumption made by Kuznetsov et al. [46] and is based on biological measurements.

### 1.4.3 Models used

In this dissertation, we develop four mathematical models to study the interaction of immune and tumour cells in body tissue.

- **Model 1-** Extension of Matzavinos et al. [6]: The first model we consider is used to study the growth, production of off spring, death and the local interaction between species. It consists of a system of five coupled ordinary differential equations that represent the rates of change of cell densities. The analysis of this model begins by collapsing it to a system of two differential

equations on the assumption that the formation of cellular conjugates occurs on a time scale of few minutes while that of tumour cells as well as the influx of immune cells into the spleen occurs on a much slower time scale, probably tens of hours [46]. Another assumption, considered also by Matzavinos et al. [6] is that the dead immune and tumour cells do not influence the formation of cellular conjugates. These two assumptions lead to two ODEs in immune and tumour cell densities. This allows us to explicitly analyse the two cell concentration competition in the body. Further, as noted by Matzavinos et al. [6], an explicit two dimensional model could be investigated.

- **Model 2-** Extension of Matzavinos et al. [6]: The second model is used to study the spatial distribution dynamics of the cell populations through reaction diffusion, which describes the random mobility of cells, and the chemotaxis phenomenon which describes the migration of immune cells towards tumour cells. It consists of three PDEs compared to the four that Matzavinos et al. [6] analysed. In simulating this model, we use finite differences. We discretize the space and time using the Crank Nicholson method which is unconditionally stable. We as well perform a travelling wave analysis on this model. We introduce immunotherapy and formulate two new models which we analyse to study the effects of immunotherapy on the cell densities.
- **Model 3-** New local kinetics model with immunotherapy: We construct a new model to incorporate immunotherapy in model 1. We then analyse this model to study the effects of immunotherapy on TICLs-tumour interaction particularly cancer dormancy.
- **Model 4-** New spatial distribution model with immunotherapy: We construct a new model by extending model 3 to consider spatial distribution,

that is diffusion of the cell densities and the cytokine we consider (IL2), and chemotaxis of TICLs.

The analytical solutions to the models we formulate are hard to get and in fact may not exist. We therefore do a linear stability analysis of the homogeneous models to predict the long term behaviour of the solutions. We study the feasibility of our models to establish whether the domains under which we assume the solutions to lie make sense and also perform a sensitivity analysis to establish the most important parameters that should be targeted in order to eliminate cancer in a human tissue. For the local kinetic interaction models, we obtain threshold conditions for the stability of healthy steady states (tumour free steady state solutions). Numerical simulations for all models (1-4) are performed to verify the theoretical results, and they also aid us in shading a big picture of what the analytical solutions can be. Matzavinos et al. [6] reduced the 6D system to a 4D system. However, for simplicity they could have further reduced it to a 2D system for the homogeneous part, and a 3D system for the non homogeneous part. It is possible that little further insight would be gained by analysing the more complex 4D model. Consequently it may be feasible to reduce the original 6D system to a 3D system by assuming that the rate of change of cell complex formation is extremely slow; the same assumption as was made by Kuznetsov et al. [46] and Fishelson et al. [50]. The models so developed would be easier to analyse, because their focus would be limited to TICLs and tumour cell densities. Similarly, Matzavinos et al. [6] did not analyse the feasibility of the domain under which the immune and tumour cell solutions are defined. In developing our new models, we introduce a new class of cells, the resting cell class from which the TICLs are recruited. Matzavinos et al. [6] considered a constant supply of TICLs into the tumour cell localization but this is not the case in real life.

## 1.5 Overview

In this Chapter, we have given a brief motivation for our research, outlined how tumours are formed and how the immune system responds to them. We reviewed some cancer modelling studies and the basic aspects we do consider in this dissertation. Tumour-immune interactions can be modelled mathematically and they have been reasonably useful, however, the phenomenon of cancer dormancy up to now is still not fully understood. So in an attempt to understand tumour-immune interactions particularly the phenomenon of cancer dormancy, we develop mathematical models to investigate the interaction between tumour cells and cytotoxic infiltrating T-lymphocytes. Understanding these interactions can possibly paint a clear picture of what cancer dormancy is. Four models are presented and studied in this dissertation: models 1 and 2 are presented in Chapters 2 and 3 respectively, and models 3 and 4 are both studied in Chapter 4. Our final conclusions and recommendations are presented in Chapter 5.

# Chapter 2

## Local kinetic interactions

In this Chapter, we investigate the dynamics of TICLs-tumour cells interaction in a spatially homogeneous domain. We present a mathematical kinetic model to study the growth, proliferation, production of offspring, and death with local interactions between tumour cells and the TICLs. We discuss its feasibility, obtain the steady states and investigate their stability. We then determine a threshold condition for the local asymptotic stability of the healthy steady state, investigate the global stability of the healthy steady state, carry out a sensitivity analysis of some of the parameters and also analyse the phase space in which the solutions to the model we formulate lie, simulate the model and finally discuss the implications of the results.

### 2.1 Model formulation

The model we consider is a slight modification of Matzavinos et al. [6]. It subdivides the cell population into local concentrations of TICLs  $E$ , tumour cells  $T$ , TICL-tumour complexes  $C$ , inactivated TICLs  $E^*$ , lethally hit or programmed for

lysis tumor cells  $T^*$  and a single chemokine  $\alpha$ . We consider a simplified process of a growing, avascular tumour that calls for a response from the host immune system and allure a population of lymphocytes. The growing tumour is directly attacked by TICLs (see [31, 40, 47]) which in turn secrete soluble diffusible factors called chemokines. These factors capacitate the TICLs to respond in a chemotactic manner and migrate towards the tumour cells. We firstly consider the local interactions involving cell proliferation for both the tumour and immune cells, formation of cell complexes and cell deaths for both tumour and immune cells. These interactions are modelled to take place in vivo. According to the scheme shown in Figure 2.1 and following the receptor-ligand kinetics theory by Lauffenburger et al. [38], when a tumour cell and a TICL cell come into contact, it may lead to formation of a TICL-tumour complex at a binding rate  $k_1$  which later can either lead to tumour cell death with a probability  $p$  and a rate  $k_2p$ , or inactivation of TICLs at a rate  $k_2(1 - p)$ . In case of the latter, the TICL-tumour complex is dissociated at a rate  $k_1$ . Here  $k_2$  is a parameter describing the rate of detachment of TICLs from tumour cells, resulting in an irreversible programming of the tumour cells for lysis. We assume that the rate of supply of immune cells into the region of tumour localization is constant  $s$ . We consider the immune cells proliferation term to be  $fC/(g + T)$ , where  $f$  and  $g$  are constant parameters derived from experimental results. Its a function that explains how tumour cells proliferates a result of interaction with immune cells. This term was first considered by Matzavinos et al. [6] in response to experimental observations on the proliferation of TICLs in response to the tumour. This functional form is in line with a model in which one presumes that the enhanced proliferation of TICLs is as a result of signals such as interleukins, generated by immune cells in tumour-TICL cell complexes (eg IL2) and act mainly in an autocrine fashion [6].

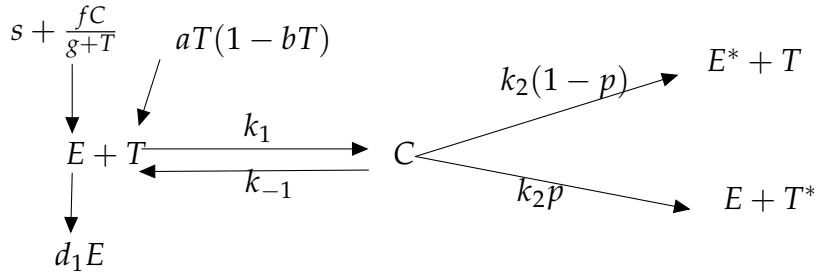


Figure 2.1: A diagram showing local interactions between T-cells and tumour cells, cells' proliferation and death.

With the above assumptions, we get the following Matzavinos et al. [6] competition model:

$$\frac{dE}{dt} = s + \frac{fC}{g+T} - d_1E - k_1ET + (k_{-1} + k_2p)C, \quad (2.1a)$$

$$\frac{dT}{dt} = aT(1 - bT) - k_1ET + (k_{-1} + k_2(1 - p))C, \quad (2.1b)$$

$$\frac{dC}{dt} = k_1ET - (k_{-1} + k_2)C, \quad (2.1c)$$

$$\frac{dE^*}{dt} = k_2(1 - p)C - d_2E^*, \quad (2.1d)$$

$$\frac{dT^*}{dt} = k_2pC - d_3T^*, \quad (2.1e)$$

where  $a$  is the intrinsic growth rate of tumour cells. It is equivalent to the natural tumour growth rate less the death rate,  $b^{-1}$  is the tumour carrying capacity,  $d_1$ ,  $d_2$  and  $d_3$  are respectively the death rate of the immune cells, and de-activation rates of the dead immune cells and dead tumour cells. All the parameter values are positive.

Table 2.1: **State variables for the tumour-immune cells model (2.1).**

State variable	Description
$E$	Concentration of TICLs in cells per centimetre.
$T$	Concentration of tumour cells in cells per centimetre.
$C$	Tumor-TICLs complexes in cells per centimetre.
$E^*$	De-activated/dead TICLs in cells per centimetre.
$T^*$	Lethally hit/dead tumour cells in cells per centimetre.

Table 2.2: **Parameter description for the tumour-immune cells interaction model (2.1).**

Parameter	Description
$k_1$	Rate of binding of TICLs to tumour cells.
$k_{-1}$	Rate of detachment of TICLs from tumour cells without damaging the cells.
$k_2$	Rate of detachment of TICLs from tumour cells resulting into cell death.
$p$	Probability of de-activating/killing tumour cells.
$k_2p$	Death rate of tumour cells.
$k_2(1 - p)$	Death rate of TICLs.
$s$	Rate of normal flow of mature cytotoxic T-lymphocytes into the tumour localisation.
$d_1$	Natural death rate of TICLs.
$d_2$	Rate of decay of de-activated TICLs.
$d_3$	Rate of decay of lethally hit/dead tumour cells.
$a$	Intrinsic tumour growth rate.
$1/b$	Tumor carrying capacity.

It is worth noting that the rate  $C$  of formation of tumour-TICL complexes is fast compared to the rate of change of TICLs and tumour cells. The formation of these cellular conjugates occurs on a time scale of several minutes to a few hours.

A time interval of this order is also observed before the programmed lysis of lethally hit tumour cells [50, 51]. However, the multiplication of immune cells into the spleen occurs on a much slower time scale, probably tens of hours. This motivates the application of a quasi-steady state approximation to (2.1c) (i.e.  $\frac{dC}{dt} \approx 0$ ) [46]. Substituting

$$\frac{dC}{dt} \approx 0 \quad \text{into the equation (2.1c),}$$

we get the following relation:  $C \approx KET$ ,

where

$$K = \frac{k_1}{k_{-1} + k_2}. \quad (2.2)$$

It is also worth noting that  $E^*$  and  $T^*$  do not in any way affect the tumour, immune cells or tumour-TICL complexes. It is therefore sufficient to analyse the dynamics of TICLs and tumour cells in equations (2.1a) and (2.1b). Equations (2.1a to e) now become simplified down to two equations

$$\frac{dE}{dt} = s + \frac{\rho ET}{g + T} - lET - d_1 E, \quad (2.3a)$$

$$\frac{dT}{dt} = aT(1 - bT) - mET, \quad (2.3b)$$

where  $\rho$ ,  $l$  and  $m$  are positive parameters such that

$$l = Kk_2(1 - p), \quad \rho = fK, \quad m = Kk_2p.$$

We start the analysis of model (2.3) by non-dimensionalizing the system of equations by setting

$$x = \frac{E}{E_0} \quad \text{and} \quad y = \frac{T}{T_0} \quad \text{and} \quad \bar{t} = \frac{t}{t_0}, \quad (2.4)$$

where  $T_0 = T(t = 0)$  and  $E_0 = E(t = 0)$ . We choose the magnitude of the TICLs and tumour concentrations to be  $E_0 = 10^6$  cells/cm and  $T_0 = 10^7$  cells/cm. This choice is motivated by the fact that a tumour nodule grows to relatively a size 1 – 3 mm in diameter, containing approximately  $10^5$  to  $10^9$  cells. This is got from clinical observations of dormant tumours [52]. The time is scaled relative to the rate of TICLs' deactivation; i.e  $t_0 = 1/d_1$ . Substituting for  $x$ ,  $y$ , and  $\bar{t}$  into the equations (2.3), we obtain a 2-dimensional system of fractional populations  $x$ , and  $y$ . For convenience, we later drop the bar on the non-dimensionalised time  $\bar{t}$ . The model (2.3) can then be re-expressed as:

$$\frac{dx}{dt} = \sigma_1 + \frac{\gamma xy}{\eta + y} - \nu xy - x, \quad (2.5a)$$

$$\frac{dy}{dt} = \beta_1 y(1 - \beta_2 y) - \mu xy, \quad (2.5b)$$

where

$$\sigma_1 = \frac{s}{E_0 d_1}, \quad \gamma = \frac{fK}{d_1} = \frac{\rho}{d_1}, \quad \eta = \frac{g}{T_0}, \quad \nu = \frac{lT_0}{d_1},$$

$$\beta_1 = \frac{a}{d_1}, \quad \beta_2 = bT_0, \quad \text{and} \quad \mu = \frac{mE_0}{d_1}.$$

In this section we have developed a simplified 2D model of tumour-TICL interaction dynamics in a homogeneous domain (without space). We next analyse the domain in which we impose the solutions, to establish whether it is feasible.

## 2.2 Boundedness and feasibility analysis

In this section we analyse the boundedness of the solutions to the system (2.5), describe the domain under which they carry meaning and analyse the feasibility

of solutions in this domain. In equations (2.5),  $x$  and  $y$  carry no physical meaning when  $x < 0$  and  $y < 0$ . For this model, there exists a domain  $\mathbb{D}$  in which the system of equations is mathematically and epidemiologically well-defined. We define this domain  $\mathbb{D}$  as

$$\mathbb{D} = \left\{ \begin{pmatrix} x \\ y \end{pmatrix} \in \mathbb{R}^2 \mid \begin{array}{l} x \geq 0, \\ y \geq 0 \end{array} \right\}.$$

**Theorem 2.1** *For the system (2.5), if the initial conditions lie in  $\mathbb{D}$ , the system of equations for the TICLS-tumour interaction model has a unique solution that exists and remains in  $\mathbb{D}$  for all  $t > 0$ .*

*Proof*

We proceed by firstly determining the nature of the trajectories on the boundary of the domain  $\mathbb{D}$ . Let  $D_1 = \{(0, y)\}$  and  $D_2 = \{(x, 0)\}$ . On  $D_1$ ,

$$\frac{dx}{dt} \Big|_{x=0} = \sigma_1 > 0 \quad \text{and} \quad \frac{dy}{dt} \Big|_{x=0} = \beta_1(1 - \beta_2 y) \geq 0.$$

On  $D_2$ ,

$$\frac{dx}{dt} \Big|_{y=0} = \sigma_1 - x \quad \text{and} \quad \frac{dy}{dt} \Big|_{y=0} = 0.$$

This implies that at the boundaries ( $\Omega_0 := \{D_1 \cup D_2 \mid x, y \in \mathbb{R}\}$ ) of the domain, the trajectories are always pointing in the positive direction or simply remain on  $D_2$ . For solutions to be negative, they must cross the boundary of the domain, but this does not happen because the trajectories remain on  $D_2$  irrespective of the value of  $\sigma_1$  (see Figure 2.2). We are therefore left to show that for the system (2.5), if the initial conditions lie in  $\mathbb{D}$ , the solutions to the system of equations for the TICLS-tumour interaction model do not blow up, that is they are bounded from above in  $\mathbb{D}$  for all  $t > 0$ .

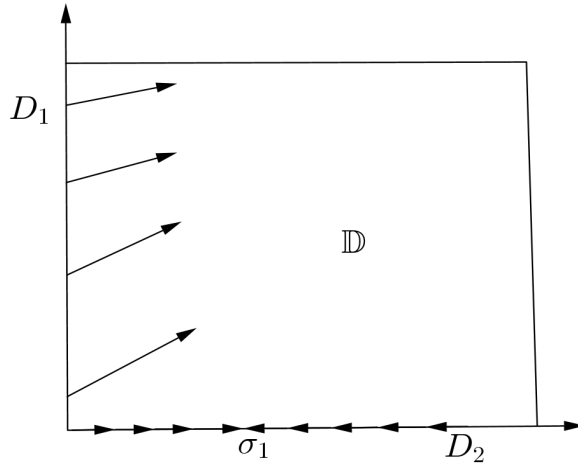


Figure 2.2: Diagram showing the direction vector field on  $D_1$  and  $D_2$ .

It is easy to see from (2.5b) that,

$$\begin{aligned} \beta_1 y(1 - \beta_2 y) - \mu xy &= \frac{dy}{dt} \leq \beta_1 y(1 - \beta_2 y), \\ \frac{1}{\beta_1} \int \frac{dy}{y} + \frac{\beta_2}{\beta_1} \int \frac{dy}{(1 - \beta_2 y)} &\leq \int dt, \\ \frac{1}{\beta_1} \ln y - \frac{1}{\beta_1} \ln |1 - \beta_2 y| &\leq t + \ln C, \\ y(t) &\leq \frac{C}{C\beta_2 + \exp(-\beta_1 t)}, \end{aligned}$$

where

$$C \geq \frac{y_0}{1 - \beta_2}, \quad y(0) = y_0 \in \mathbb{D}. \quad \text{Taking limits on both sides as } t \text{ tends to infinity,}$$

$$\lim_{t \rightarrow \infty} y(t) \leq \frac{1}{\beta_2}.$$

This also confirms that  $y(t)$  is bounded from above by  $1/\beta_2$ .

From equation (2.5a) and taking into consideration that

$$\lim_{t \rightarrow \infty} y(t) \leq \frac{1}{\beta_2},$$

$$\frac{dx}{dt} \leq \sigma_1 + \gamma_0 \bar{y} x - \nu x \bar{y} - x,$$

where

$$\bar{y} = \frac{1}{\beta_2}, \quad \text{and} \quad \gamma_0 = \frac{\gamma\beta_1}{\eta\beta_1 + 1}.$$

By the boundedness of  $y$ , and using the inequality theorem,

$$\begin{aligned} \frac{dx}{dt} &\leq \sigma_1 + (\gamma_0\bar{y} - (\nu\bar{y} + 1))x, \\ \int \frac{dx}{\sigma_1 + (\gamma_0\bar{y} - (\nu\bar{y} + 1))x} &\leq \int dt, \\ \frac{1}{\gamma_0\bar{y} - (\nu\bar{y} + 1)} \ln \left| \frac{\sigma_1 + (\gamma_0\bar{y} - (\nu\bar{y} + 1))x}{K} \right| &\leq t, \\ x(t) &\leq \frac{K \exp -((\nu\bar{y} + 1) - \gamma_0\bar{y}) - \sigma_1}{\gamma_0\bar{y} - (\nu\bar{y} + 1)}. \end{aligned}$$

Taking the limit as time tends to infinity,

$$\lim_{t \rightarrow \infty} x(t) \leq \frac{\sigma_1}{\nu\bar{y} + 1 - \gamma_0\bar{y}}.$$

This as well confirms that  $x(t)$  is bounded from above provided that

$$\frac{\nu\bar{y} + 1}{\gamma_0\bar{y}} > 1.$$

■

We have proved that our solutions are bounded and also shown that the domain  $\mathbb{D}$  is positively invariant. In fact for all  $t \geq 0$ ,

$$0 \leq x(t) \leq \frac{\sigma_1}{\nu\bar{y} + 1 - \gamma_0\bar{y}} \quad \text{and} \quad 0 \leq y(t) \leq \frac{1}{\beta_2}.$$

We now next investigate the steady state solutions of the model (2.5).

## 2.3 Steady state solutions and stability analysis

The solutions to the model (2.5) are analytically hard to find. We therefore determine the steady state solutions to observe the nature of the solutions for large

times. We obtain the steady states by equating equations (2.5a) and (2.5b) to zero and solving them simultaneously. The model (2.5) has four solutions: one healthy steady state

$$X^0 = \begin{pmatrix} x \\ y \end{pmatrix} = \begin{pmatrix} \sigma_1 \\ 0 \end{pmatrix}, \quad (2.6)$$

and the three other solutions are the roots of the equation

$$\beta_1\beta_2\nu y^3 + \xi_1 y^2 + y + \xi_2\sigma_1\eta + \beta_1\gamma - \beta_1\gamma = 0, \quad (2.7)$$

where

$$\xi_1 = (\beta_1\beta_2\gamma\eta + \beta_1\beta_2 - \beta_1\nu) \quad \text{and} \quad \xi_2 = (\sigma_1\mu - \beta_1\beta\gamma - \beta_1\gamma\eta + \beta_1\beta_2\eta).$$

With the parameter values defined in Table 2.3, equation (2.7) has three roots, two of which are biologically meaningless because they are negative and do not lie in the domain of interest  $\mathbb{D}$ . The third steady state that lies in  $\mathbb{D}$  is

$$X^1 \approx \begin{pmatrix} x \\ y \end{pmatrix} \approx \begin{pmatrix} 5.8998 \\ 0.91938 \end{pmatrix}. \quad (2.8)$$

By linearising the system (2.5) about the steady states, we obtain the linear systems

$$\frac{dX}{dt} = Df(X^0) \quad \text{and} \quad \frac{dX}{dt} = Df(X^1),$$

where  $Df(X^0)$  and  $Df(X^1)$  are Jacobian matrices evaluated at  $X^0$  and  $X^1$  respectively. For  $Df(X^0)$ , there are two eigenvalues,  $\lambda_1 = -1$  and  $\lambda_2 = 41.2$ , implying that the healthy (tumour free steady state) is unstable. For  $Df(X^1)$ , there are two complex eigenvalues,  $\lambda_{1,2} = -0.43 \pm 5.26i$  with negative real parts. This means that  $X^1$  is a stable focus, implying that the steady state representing tumour dormancy is stable. This is in line with findings in Matzavinos et al. [6]. This steady state analysis explains tumour dormancy, a situation where tumour cells neither

do proliferate nor die. The tumour dormant state is stable implying that a person can indeed live with a tumour in this sort of state for his or her entire life time. We next formulate a threshold condition for the stability of the healthy steady state.

### 2.3.1 Threshold condition

We obtain a threshold condition for the stability of the tumour free equilibrium state (TFE). We do this to establish a condition that should be strived for in order to eradicate tumour cells in a human body. We obtain this threshold from the Jacobian of the system (2.5) at the TFE (2.6) and on the assumption that all parameter values are positive. The stability of the three other solutions depends on all the parameter values.

$$J_{E_0} = DV(E_0) = \begin{pmatrix} -1 & 0 \\ 0 & \beta_1 - \mu\sigma_1 \end{pmatrix}. \quad (2.9)$$

For the TFE to be locally asymptotically stable, the eigenvalues of the Jacobian matrix (2.9) should be negative or should have negative real roots. It is however trivial to show that the characteristic equation of the Jacobian matrix (2.9) can not have complex roots. It can however have negative eigenvalues only if  $\beta_1 < \mu\sigma_1$ . We therefore define the threshold to be;

$$R_0 := \frac{\beta_1}{\mu\sigma_1} = \frac{ad_1(k_{-1} + k_2)}{k_1k_2p}. \quad (2.10)$$

The TFE (2.6) is locally stable if  $R_0 < 1$  (see van den Drische et al. [53]). Our analysis suggests that, in order for the TICLs to out-compete the tumour cells in the body tissue,  $R_0 < 1$ . In (2.10), it is evident that parameter values that need

to be kept low are the intrinsic tumour growth rate  $a$ , the rate of natural death of TICLs  $d_1$ , and the rate of detachment of TICLs from tumour cells  $k_{-1}$  while those that should be kept high are rate of detachment of TICLs from tumour cells resulting in an irreversible tumour cells for lysis  $k_2$ , probability of killing tumour cells  $p$  and the rate of binding of TICLs to tumour cells  $k_1$ . These all make sense. For example, immunotherapy, chemotherapy, surgery or other suitable interventions, will target increasing tumour cell death thus reducing the intrinsic rate of growth of tumour cells and also increasing the number of immune cells. This portrays a clear picture that it is hard to have  $R_0 < 1$  and therefore hard to have a tumour free steady state (eliminate cancer in a human body) because some of the parameters in equation 2.10 that should be targeted for example  $a$ , the intrinsic tumour growth rate and  $d_1$ , the natural death rate of TICLs are hard to actually in any way be altered by any form of cancer treatment.

### 2.3.2 Investigating global stability of the TFE

In this section, we investigate the stability of the TFE. From van den Driische et al. [53], we know that the tumour free equilibrium point is locally asymptotically stable if and only if  $R_0 < 1$ . We investigate global stability using a theorem by Castillo-Chavez et al. [54].

**Theorem 2.2** *For a system*

$$\begin{aligned}\frac{dX}{dt} &= F(X, Z), \\ \frac{dZ}{dt} &= G(X, Z), \quad G(X, 0) = 0,\end{aligned}$$

where the components of the column vector  $X \in \mathbb{R}^m$  denote the number of uninfected classes and the components of the vector  $Z \in \mathbb{R}^n$  denote the number of infected classes

and  $U_0 = (X^*, 0)$  denotes the disease free equilibrium of the system, the fixed point  $U_0 = (X^*, 0)$  is globally asymptotically stable if  $R_0 < 1$  and the following two conditions are met:

1. For  $\frac{dX}{dt} = F(X, 0)$ ,  $X^*$  is globally asymptotically stable,
2.  $G(X, Z) = AZ - \hat{G}(X, Z)$ ,  $\hat{G} \geq 0$  for  $X, Z \in \Omega$ , where  $A = D_Z G(X^*, 0)$  is an M-matrix (the off diagonal elements of  $A$  are non negative) and  $\Omega$  is the region where the model makes biological sense. If the system satisfies the the above two conditions, then the fixed point  $U_0 = (X^*, 0)$  is globally asymptotically stable provided  $R_0 < 1$ .

*Proof*

For simplicity, we write the system (2.5) using the notation in Theorem 2.2 above;

$$X = (x) \quad \text{and} \quad Z = (y),$$

and

$$F = \left( \sigma_1 + \frac{\gamma xy}{\eta + y} - \nu xy - x \right),$$

$$G = (\beta_1 y(1 - \beta_2 y) - \mu xy).$$

It follows that

$$\hat{G}(X, Z) = D_Z G_{E_0} Z - G(X, Z) = \left( (\beta_1 - \frac{\mu}{\sigma_1})y - \beta_1 y(1 - \beta_2 y) + \mu xy \right) \not\geq 0 \quad (2.11)$$

using the parameter values in Table 2.3. We note that the TFE point (2.6) is **not globally** asymptotically stable. ■

This indicates that in case one has a tumour, it is impossible for them to achieve a TFE and it lasts forever (situation where they are tumour free). In this section,

we calculated a threshold condition  $R_0$  and showed that for the tumour free equilibrium steady state (TFE) to be locally asymptotically stable,  $R_0 < 1$ . We also showed that the TFE is not globally stable implying that its impossible to achieve it. In the next section, we investigate the most important parameter values that influence the phase space of model (2.5).

## 2.4 Sensitivity and phase space analysis

The parameter values defined in Section 2.1 are only baseline values. In this section we investigate critical parameter values that have an effect on the system of equations (2.5). We also analyse the phase space of the solutions to the system (2.5). Firstly, we analyse the phase space of the system by investigating whether it has a limit cycle or not. In the model considered by Matzavinos et al. [6], they found that their system had closed orbits. In this case however, we prove that the system has no closed orbits.

**Theorem 2.3** *The system (2.5) has no closed orbits for positive values of  $x$  and  $y$ .*

**Theorem 2.4** *We use Dulac's criterion [55] as follows.*

*Let  $\mathbb{D}$  be a simply connected region of the  $x - y$  plane and*

$$\frac{dx}{dt} = f(x, y), \quad (2.12a)$$

$$\frac{dy}{dt} = g(x, y) \quad (2.12b)$$

*be a dynamical system in which  $f$  and  $g$  are continuously differentiable. If there exists a continuously differentiable function  $\phi(x, y)$  such that*

$$\frac{\partial}{\partial x} \{ \phi(x, y) f(x, y) \} + \frac{\partial}{\partial y} \{ \phi(x, y) g(x, y) \}$$

is of a constant sign in  $\mathbb{D}$ , then the system (2.12) has no closed orbits wholly contained in  $\mathbb{D}$ .

*Proof*

To prove that our system (2.5) has no closed orbits (limit cycle), we consider

$$\phi(x, y) = \frac{1}{xy},$$

$$\begin{aligned} \nabla \cdot (\phi(x, y)\dot{X}) &= \frac{\partial}{\partial x} (\phi(x, y)f(x, y)) + \frac{\partial}{\partial y} (\phi(x, y)g(x, y)), \\ &= \frac{\partial}{\partial x} \left( \frac{\sigma_1}{xy} - \frac{\gamma}{\eta + y} - \nu - \frac{1}{y} \right) + \frac{\partial}{\partial y} \left( \frac{\beta_1}{x}(1 - \beta_2 y) - 1 \right), \\ &= - \left( \frac{\sigma_1}{x^2 y} + \frac{\beta_1 \beta_2}{x} \right). \end{aligned}$$

since  $\beta_1, \beta_2$  and  $\sigma_1$  are all positive, this implies that  $\nabla \cdot (g\dot{X}) < 0 \forall x, y \in \mathbb{D}$ , where

$$\mathbb{D} = \left\{ \left( \begin{array}{c} x \\ y \end{array} \right) \in \mathbb{R}^2 \mid \begin{array}{l} x \geq 0, \\ y \geq 0 \end{array} \right\}.$$

■

From the threshold condition (2.10) given in Section 2.3.1, we choose to analyse the nature of the phase space for high and low values of  $\sigma_1$  and  $\mu$ . These are the parameter values that any form of cancer treatment will have to target. The other parameter values are set to be fixed by taking those in Table 2.3. By using *PPLANE 2005.10*, a software package that uses *MATLAB* to sketch phase portraits for 2D systems, we plot values of  $x$  against  $y$  for low and high values of  $\sigma_1$  and  $\mu$ . This is shown for the ODE system (2.5) in figures 2.4. We also use parameter values in Table 2.3 to plot the phase portrait of  $y$  the fractional tumour density against  $x$ , the fractional TICLs cell density in Figure 2.3.

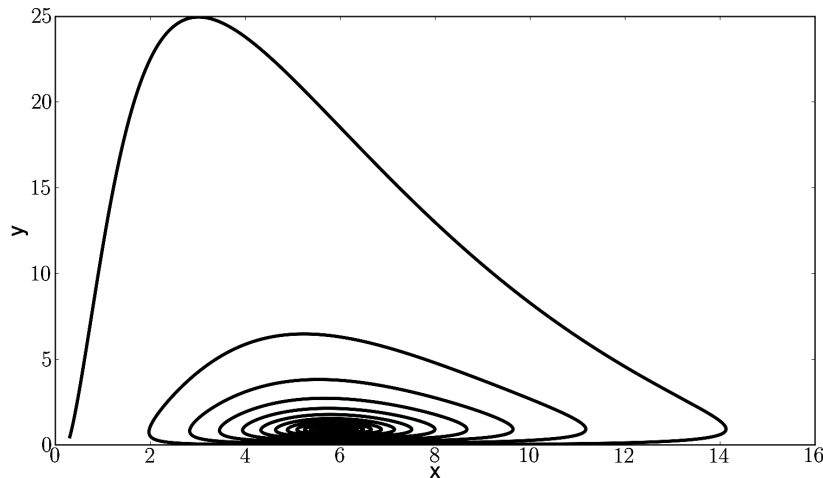


Figure 2.3: **Phase space of the ODE system (2.5). The phase plane is a stable focus converging to the tumour dormant state.**

Figure 2.3 shows the phase space of the ODE system (2.5). It shows that the  $x$  and  $y$  solutions spiral to a stable steady state. Figures 2.4(c & d) show that lower values of  $\mu$  are desirable for TICLs to out number tumour cells. Low or high values of  $\sigma_1$  seem not to have a significant effect on the structure of the phase space (see Figures 2.4(a & b)). In this section we have highlighted the parameter values that are more responsive in eliminating cancer. We have also analysed the nature of the phase space by proving that there are no periodic solutions, contrary to what Matzavinos et al. [6] found in their model and the solutions spiral to a cancer dormant state which explains cancer dormancy. In the next section we discuss numerical simulations of the model (2.5) to determine whether they correspond to the theoretical results that we have established.

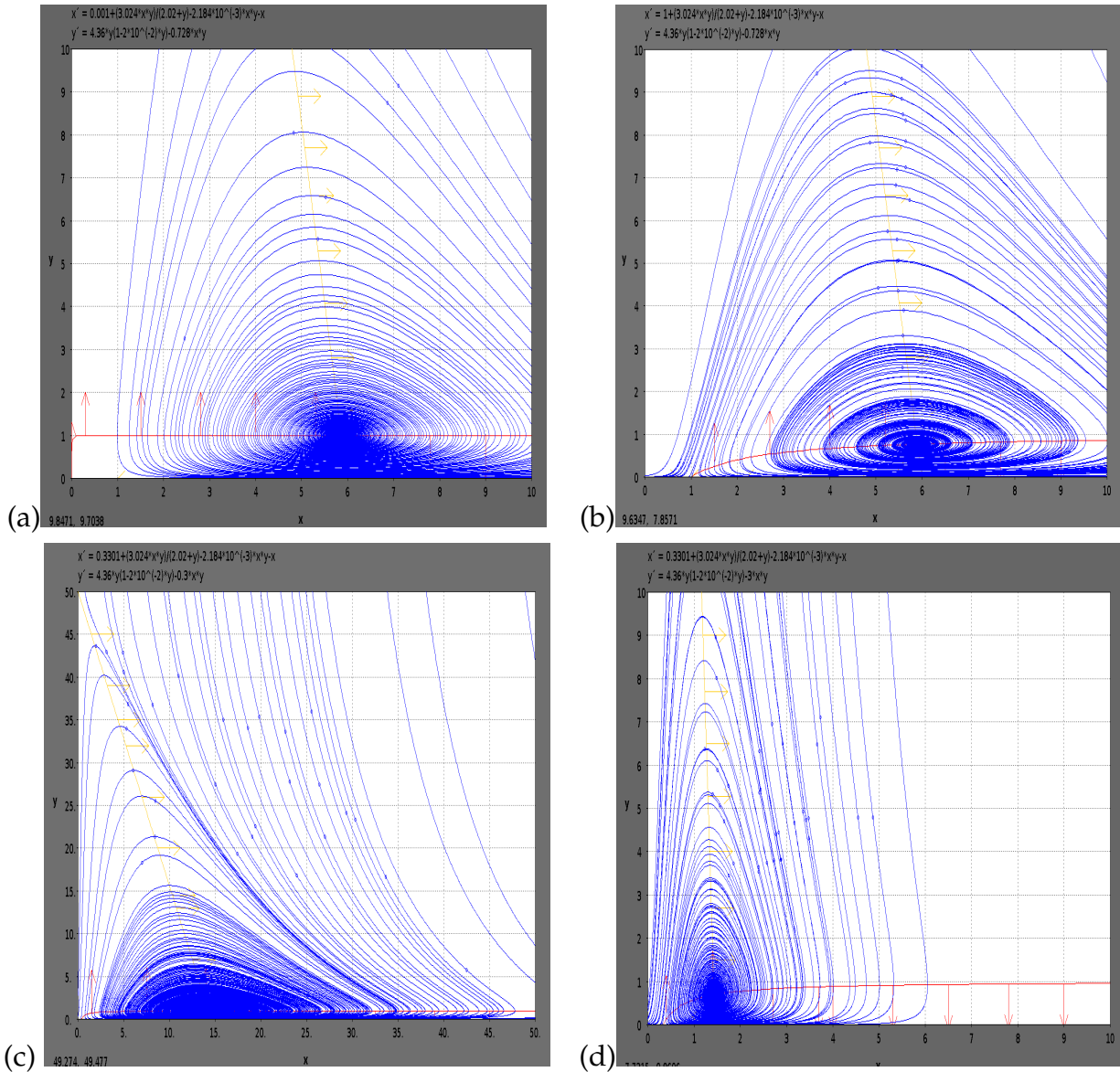


Figure 2.4: Phase plots showing the direction fields corresponding to parameter values (a)  $\sigma_1 = 0.001$ , (b)  $\sigma_1 = 1$ , (c)  $\mu = 0.3$  and (d)  $\mu = 3$  respectively.

Table 2.3: **Dimensional parameter values obtained from Matzavinos et al. [6].**

Parameter	Estimated value	Units
$a$	0.18	day <sup>-1</sup>
$k_1$	$1.3 \times 10^{-7}$	day cells <sup>-1</sup> cm
$k_2$	7.2	day <sup>-1</sup>
$d_1$	0.0412	day <sup>-1</sup>
$g$	$2.02 \times 10^7$	cells cm <sup>-1</sup>
$b$	$2.0 \times 10^{-9}$	cells <sup>-1</sup> cm
$k_{-1}$	24	day <sup>-1</sup>
$p$	0.9997	dimensionless
$f$	$0.2988 \times 10^8$	day <sup>-1</sup> cells cm <sup>-1</sup>
$s$	$1.36 \times 10^4$	day <sup>-1</sup> cells cm <sup>-1</sup>

## 2.5 Numerical simulations

We simulate the model (2.5) using the parameter values given in Table 2.3 with initial conditions  $x(0) = 0.3$  and  $y(0) = 0.5$ . The Parameter values are obtained from experimental data on Marine B cell lymphoma(BCL<sub>1</sub>) [56]. This cell was used to model tumour dormancy in a mouse [56, 57]. In the experiments, CD8+ T cells were enhanced with anti-Id antibodies into inducing dormancy by secreting Interferon-gamma (INF- $\gamma$ ), a dimerized soluble cytokine that is the only member of the type II class of interferons. The non-dimensionalized parameter values were obtained from the dimensionalised parameter values in Table 2.3 together with  $K = 4.17 \times 10^{-9}$  cm/cell,  $\rho = 0.1246$  day<sup>-1</sup>,  $l = 9 \times 10^{-12}$  cm·(cells·day)<sup>-1</sup>,  $m = 3.0 \times 10^{-8}$  cm·(cells·day)<sup>-1</sup>.

Using the non-dimensionalized parameter estimates and initial values of  $x$  and  $y$  as 0.3 and 0.5 respectively, four steady state solutions were obtained and two of

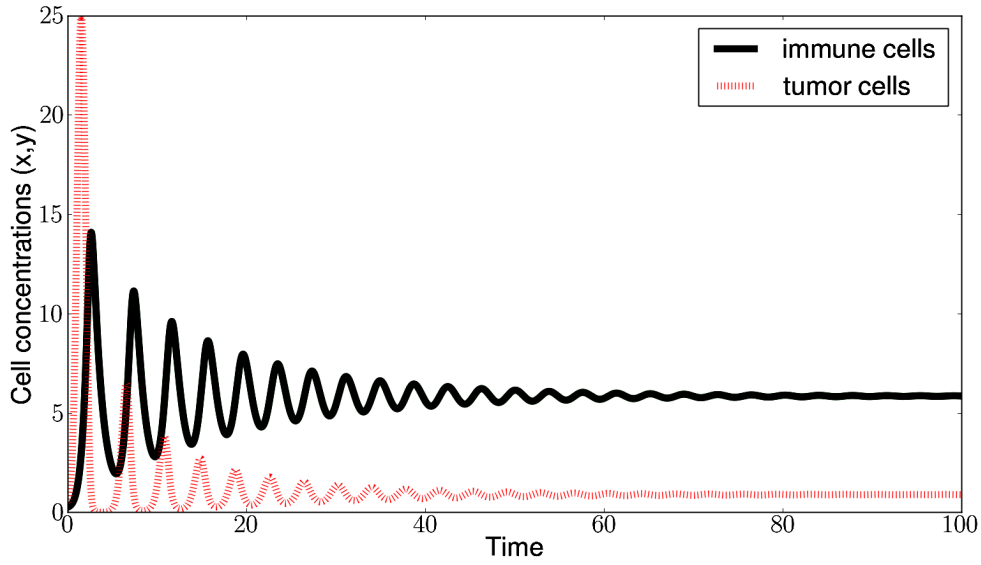


Figure 2.5: Plots of cell densities against non-dimensional time.

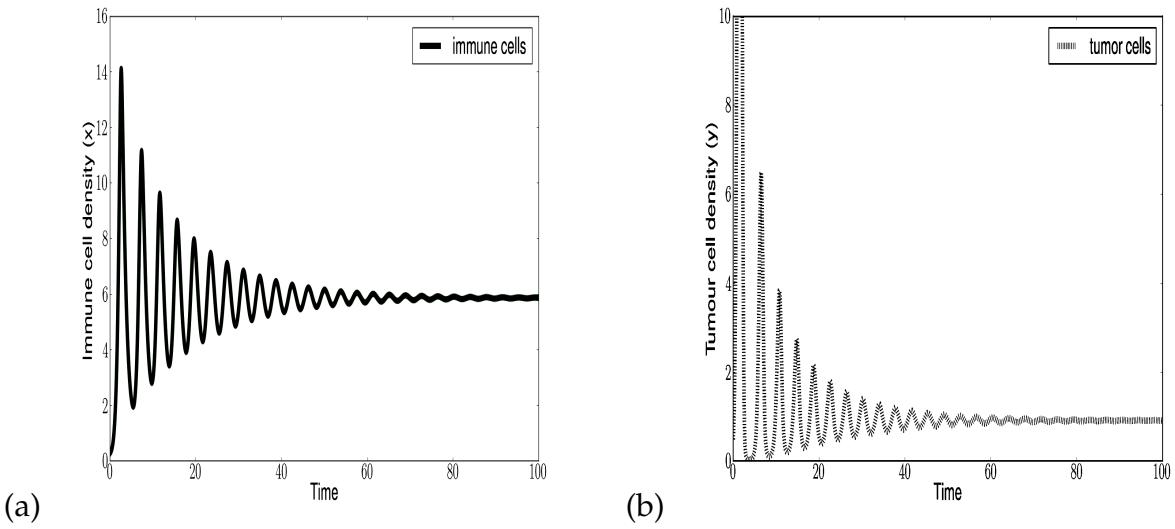


Figure 2.6: Plots of immune (TICLs) and tumour cell densities against non-dimensional time time on different scales. .

them are negative. Since we are dealing with cell densities, these two negative steady states are meaningless. The two steady states are;

$$A = (0.3301, 0) \quad \text{and} \quad B = (5.8998, 0.91938),$$

where  $A(0.3301, 0)$  represents a tumour-free unstable (saddle point) equilibrium state and  $B(5.8998, 0.91938)$  represents a tumour dormancy stable (spiral sink) state just as discussed in Section 2.3. Our analysis suggests that without any form of intervention, TICLs alone cannot completely eradicate the tumour. However, TICLs keep the tumour at some dormant state. From our theoretical results, the tumour free equilibrium steady state can only be locally asymptotically stable if  $R_0 < 1$ . The baseline values used do not however satisfy this condition. Figure 2.5 represents a cancer dormancy state, a state where the tumour cells' proliferation and death balances. It represents the steady state solution B. It shows that the immune cells outnumber the tumour cells but do not completely deactivate or kill all the tumour cells. In fact, without intervention, the disease is not eradicated from the tissue. Figure 2.6 shows the variation of TCILs and tumour cells with time on different scales. These Figures were obtained by simulating the model (2.5) using Euler's numerical scheme with  $n$ , the number of iterations equal to 20,000. We implemented this in *PYTHON* software.

In Section 2.4, we performed a sensitivity analysis to determine the quantitative change in the behaviour of the solutions in response to change in the parameter values that form the threshold (2.10) that we found in Section 2.3.1. We showed that  $\mu$  has a significant effect on the solutions to (2.5). Contour plots (Figures 2.7 (a) and (b)) show the effect of  $\sigma_1$  and  $\mu$  on the basic reproduction ratio  $R_0$ . From Figure 2.7 (a), we note that in order for the basic reproduction ratio to be minimized,  $\mu$  and  $\sigma_1$  should be maximized. From 2.7 (b), we note that a small basic reproduction ratio requires  $\beta_1$  to be minimized and  $\mu$  to be maximized. This

is in line with what we earlier found in Section 2.3. We noted earlier in Section 2.3.1, that for a tumour free equilibrium steady state to be locally asymptotically stable,  $R_0 = \beta_1/\sigma_1\mu < 1$ . Thus we should endeavour to maximize  $\sigma_1$  and  $\mu$  in order to lower  $R_0$ . This implies that indeed, the natural tumour growth rate  $a$ , the rate of natural death of TICLs  $d_1$ , and the rate of detachment of TICLs from tumour cells  $k_{-1}$  should be reduced whereas the rate of detachment of TICLs from tumour cells resulting in an irreversible tumour cells for lysis  $k_2$ , probability of killing tumour cells  $p$  and the rate of binding of TICLs to tumour cells  $k_1$  should be kept high by any cancer intervention.

In this Chapter we developed a 2D model to explicitly analyse the dynamics of tumour and TICLs in a homogeneous domain. We did this by slightly modifying Matzavinos et al. [6] model. This we did by assuming that the rate of formation of tumour-TICL complexes is too low. We in sections 2.1 and 2.2, non dimensionalized the model (2.3), formulated a domain under which the solutions to our model lie, and discussed the feasibility of the solutions to it. In Section 2.3, we obtained the steady state solutions and investigated their stability. We obtained a cancer dormant state which is stable. We furthermore determined a threshold condition for the local asymptotic stability of the healthy steady state and investigated the global stability of the healthy steady state. We found out that the healthy steady state is not globally stable implying that it may be hard to actually eradicate a tumour in a human body. We carried out a sensitivity analysis of some of the parameters to the model in Section 2.4. We simulated the model and lastly, we discussed the implications of the results in Section 2.5. In the next Chapter, we analyse the model (2.5) in a spatially heterogeneous domain.

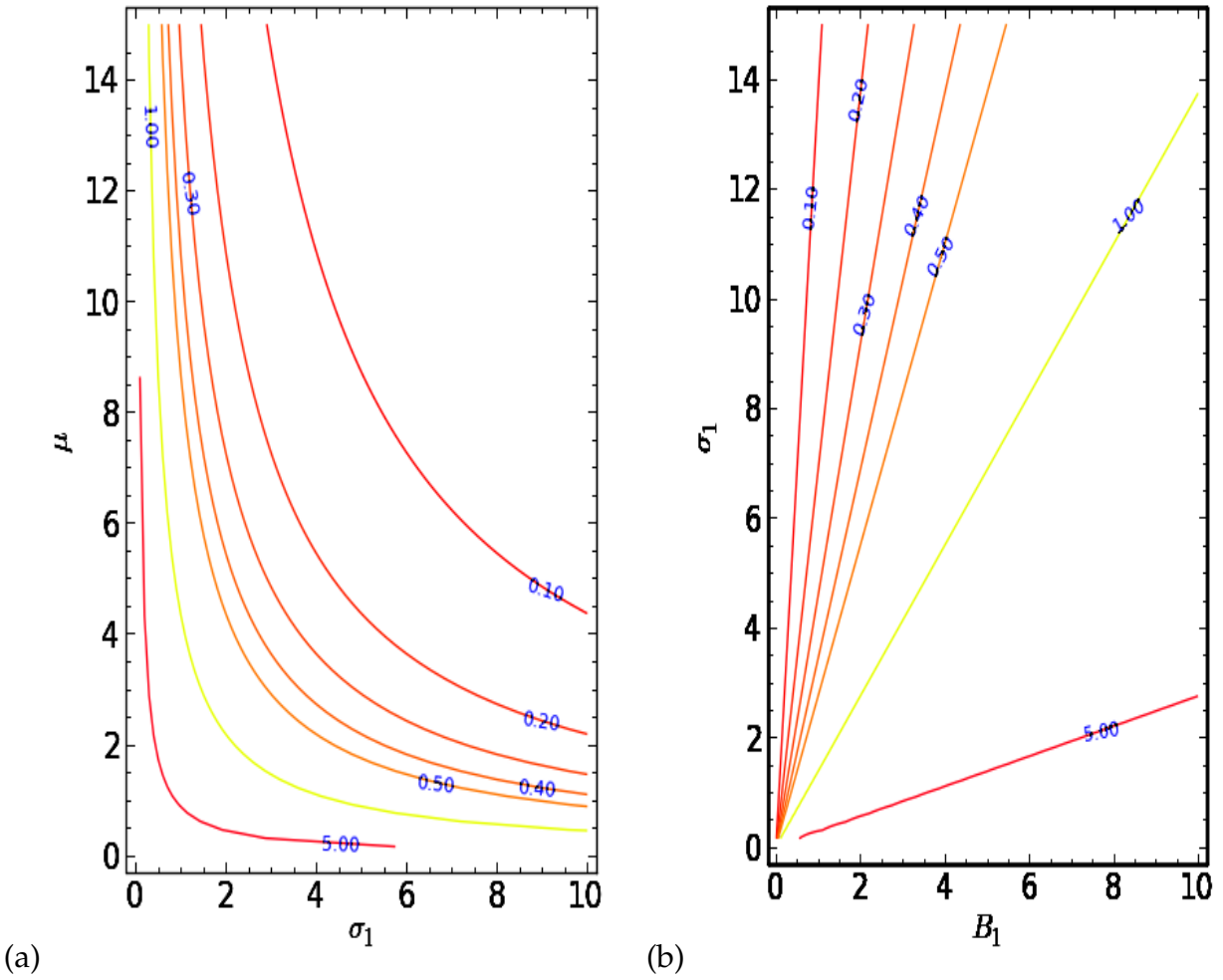


Figure 2.7: Contour plots showing the effect of the parameters  $\sigma_1$ ,  $\beta_1$  and  $\mu$  as  
(a)  $\sigma_1$  and  $\mu$  change, with  $\beta_1$  fixed. (b)  $\beta_1$  and  $\mu$  change, with  $\sigma_1$  fixed.

# Chapter 3

## Spatially heterogeneous model

In this Chapter, we investigate the dynamics of TICLs-tumour interaction in a spatially heterogeneous domain. We present a mathematical model which takes into account the local interaction kinetics, the diffusion of TICLs and tumour cells, and the chemotactic movement of the TICLs towards the tumour. We use the Crank Nicholson scheme to simulate the resulting system of PDEs. We perform a travelling wave analysis and discuss the implications of such solutions. Finally, we explain the possible implications of the results.

### 3.1 Introduction

Diffusion in the context of this study describes the random movement of both the TICLs and the tumour cells whereas chemotaxis describes the movement of the TICLs towards the tumour nodule. When an immune cell interacts with a tumour cell, it sends a signal to other cells in the form of a chemokine. The chemokine distributes in the body with different concentration gradients. Other immune cells in the body react to the signal by moving towards the area with a

high concentration of the chemokine. This process is referred to as chemotaxis. Hence chemotaxis is the phenomenon whereby somatic cells, bacteria, and other single-cell or multicellular organisms direct their movements according to certain chemicals in their environment. The model presented here is an extension of Matzavinos et al. [6] and focusses on the initial avascular stage of tumour growth. Below is a brief description of the variables in the model.

### 1. Tumour infiltrating cytotoxic lymphocytes

In addition to cell proliferation, local kinetic terms, source term, and TICLs death, we assume that the individual TICLs have an element of random mobility. We also assume that they respond to the chemokine elicited by a corresponding immune cell, thus moving chemotactically. In this model we include a TICL space competition function. This models the existence of a subregion of the domain of interest where initially there are only tumour cells and where lymphocytes do not reside as in Matzavinos et al. [6]. With all these assumptions, the partial differential equation describing the dynamics of TICLs is

$$\frac{\partial E}{\partial t} = D_1 \nabla^2 E - \chi \nabla \cdot (E \nabla \alpha) + \frac{\rho ET}{g + T} + sh(x) - lET - d_1 E, \quad (3.1)$$

where  $h(x)$  is the Heaviside function to incorporate space competition for TICLs,  $D_1$  is the diffusion coefficient which we assume to be constant,  $\chi$  is the chemotaxis coefficient, and  $\alpha$  is the chemokine concentration elicited by the immune cells. The parameters  $\chi$ ,  $l$ , and  $d_1$ , are all positive.

### 2. Tumour cell concentration

It is difficult to incorporate all the observed experimental results into a mathematical model even for an avascular tumour. However, a realistic tumour

growth model should include certain non uniformities in the central processes of inhibition of mitosis, consumption of nutrients, cell proliferation, dependence of cell mitotic rate of growth inhibitor concentration, geographical constraints as well as central Chaplain [9]. In our model, we consider diffusion of tumour cells to be linear and therefore the diffusivity is a linear constant. According to Kyle et al. [58], the rate at which tumour cells destroy the extracellular matrix is slow, this allows for lymphocytes to migrate into the tumour tissue faster than in normal tissue that has regular extracellular matrix. In addition to the population growth model in Chapter 2, we add a reaction diffusion equation to incorporate the random mobility of the tumour cells. Putting together all the above assumptions, The partial differential equation describing the dynamics of tumour cell density is

$$\frac{\partial T}{\partial t} = D_2 \nabla^2 T + aT(1 - bT) - mET, \quad (3.2)$$

where  $D_2$  is the diffusivity of the tumour cells. The parameters  $a$ ,  $b$ , and  $m$  are all positive.

### 3. Tumor-TICL complexes

We assume that there is no diffusion of complexes and therefore, we only have interactions defined by the local kinetics discussed in Chapter 1 (see [6]). The absence of diffusion is justified by the large difference in time scales for the two densities. The formation and dissociation of complexes occurs on a time scale of minutes, whereas diffusion of tumour cells and immune cells occurs on a time scale of hours. The above assumptions give the partial differential equation

$$\frac{\partial C}{\partial t} = k_1 ET - (k_{-1} + k_2 p)C. \quad (3.3)$$

However, since the formation of tumour-TICL complexes takes place in minutes, and that of immune and tumour cells requires tens of hours, we assume a quasi-steady state approximation so that

$$C = KET, \quad K = \frac{k_1}{k_{-1} + k_2}$$

as used in the previous Chapter.

#### 4. Chemokine concentration

The production of chemokines in a tumour nodule is a dynamic, multi-step process and the precise role of chemokines in tumour expansion is still not clearly understood [48]. We assume that the rate of chemokine production is proportional to tumour cell-TICLs complex density  $C$ . This is because we assume that chemokines are produced when TICLs are activated by tumor cell-TICL interactions. We also assume that the chemokines diffuse throughout the tissue at a constant diffusion rate. The above assumptions lead to the partial differential equation governing chemokine concentration as

$$\frac{\partial \alpha}{\partial t} = D_3 \nabla^2 \alpha + nET - d_4 \alpha, \quad (3.4)$$

where  $D_3$  is the diffusivity of the chemokine concentration,  $d_4$  is the deactivation rate of the chemokine concentration,  $n = Kk_3$ , and  $k_3$  is the chemokine production rate. The parameters  $n$ ,  $k_3$ ,  $D_3$  and  $d_4$  are all positive.

#### 5. Inactivated TICLs and lethally hit cells

We assume that the dead cells are eliminated from the tissue and do not much influence the immune processes. The inactivated cells also do not move. These assumptions lead to the equations

$$\frac{\partial E^*}{\partial t} = lET - d_2E^*, \quad (3.5)$$

$$\frac{\partial T^*}{\partial t} = mET - d_3E^*, \quad (3.6)$$

where  $d_2$  and  $d_3$  are deactivation rates of the lethally hit and dead tumour cells respectively.  $l$ ,  $m$ ,  $d_2$  and  $d_3$  are positive parameters. Equations (3.5), and (3.6) are coupled to the system through the tumour-TICL complexes and neither  $E^*$  nor  $T^*$  have any effect on the variables  $E$ ,  $T$  and  $C$ .

All the given assumptions together give the following system of non-linear partial differential equations:

$$\frac{\partial E}{\partial t} = D_1 \nabla^2 E - \chi \nabla \cdot (E \nabla \alpha) + \frac{\rho ET}{g + T} + sh(x) - lET - d_1 E, \quad (3.7a)$$

$$\frac{\partial T}{\partial t} = D_2 \nabla^2 T + aT(1 - bT) - mET, \quad (3.7b)$$

$$\frac{\partial \alpha}{\partial t} = D_3 \nabla^2 \alpha + nET - d_4 \alpha. \quad (3.7c)$$

For simplicity, we consider the case of one-dimensional tumour growth. The one-dimensional version of (3.1)-(3.4) does not capture the true evolution of cancer in a human body because the true geometry is complicated. Nevertheless, our major objective is to first understand the dynamics of the model in a one-dimensional setting. Later this could be extended to higher dimensions. The Heaviside function  $h(x)$  models the existence of a subregion of the domain of interest where TICLs do not reside and which is permeated by the immune cells throughout the process of diffusion and chemotaxis [6]. We define a one dimensional spatial domain to be the interval  $[0, x_0]$ , and assume that there are two regions in this interval. One fully occupied by tumour cells, the other is fully occupied by the

TICLs. We propose that the initial interval of tumour localization is  $[0, L]$ , where  $L = 0.2x_0$  (see Matzavinos et al [6]). The function  $h(x)$  is therefore defined as

$$h(x) = \begin{cases} 0 & \text{if } x - L \leq 0 \\ 1 & \text{if } x - L > 0. \end{cases}$$

## 3.2 Boundary and initial conditions

We close the system by imposing Neumann zero flux boundary conditions on the variables  $E$ ,  $T$ , and  $\alpha$ . The boundary conditions for the model (3.7) are therefore;

$$\mathbf{n} \cdot \nabla E = \mathbf{n} \cdot \nabla T = \mathbf{n} \cdot \alpha = 0. \quad (3.8)$$

We use the initial conditions considered by Matzavinos et al. [6]. The initial conditions for the model (3.7) are;

$$E(x, 0) = \begin{cases} 0, & 0 \leq x \leq L \\ E_0[1 - \exp(-1000(x - L)^2)], & L \leq x \leq x_0 \end{cases} \quad (3.9)$$

$$T(x, 0) = \begin{cases} T_0[1 - \exp(-1000(x - L)^2)], & 0 \leq x \leq L \\ 0, & L \leq x \leq x_0 \end{cases} \quad (3.10)$$

$$\alpha(x, 0) = 0 \quad \forall x \in [0, x_0]. \quad (3.11)$$

## 3.3 Parameters estimation

In addition to the parameter values that were given in Table 2.3, the set of new parameter values used, their standard units and sources are presented in Table

3.1.

Table 3.1: **Parameter values for diffusion and chemotaxis.**

Parameter	Estimated value	Units	Source
$D_1$	$10^{-6}$	$\text{cm}^2 \text{ day}^{-1}$	[6]
$D_2$	$10^{-6}$	$\text{cm}^2 \text{ day}^{-1}$	[6]
$D_3$	$10^{-4}$	$\text{cm}^2 \text{ day}^{-1}$	[6]
$k_3$	20 – 3000	molecules $\text{cell}^{-1} \text{ min}^{-1}$	[6]
$\chi$	$1.728 \times 10^6$	$\text{cm}^2 \text{ day}^{-1} \text{ moles}^{-1} \text{ cells cm}^{-1}$	[59]
$d_4$	$1.55 \times 10^{-2}$	$\text{day}^{-1}$	[60]

### 3.4 Non-dimensionalization of equations

We non-dimensionalize the system (3.7) by scaling each concentration variable using fractional quantities and letting;

$$\bar{E} = \frac{E}{E_0}, \quad \bar{T} = \frac{T}{T_0}, \quad \bar{C} = \frac{C}{C_0}, \quad \bar{\alpha} = \frac{\alpha}{\alpha_0}, \quad \bar{x} = \frac{x}{x_0}, \quad \text{and} \quad \bar{t} = \frac{t}{t_0},$$

where  $E_0 = 3.3 \times 10^5 - 10^6$  cells/cm, and  $T_0 = 10^7 - 0.5 \times 10^9$  cells/cm. Time is scaled relative to immune cell death, ie  $t_0 = x_0/D_1$ . It is worth noting that the initial TICLs and tumour cell densities make sense because, as noted earlier a human body can contain between  $10^5$  and  $10^9$  cells  $\text{cm}^{-1}$ . The chemokine concentration is normalized through some reference concentration which in our case we take to be  $10^{-10}$ , a value also considered by Nomiyama et al. [61]. The space variable  $x$  is scaled relative to the length under consideration (i.e.  $x_0 = 1$  cm) [61]. On making the above substitutions and dropping the bar on  $t$  for convenience, the model (3.7) becomes

$$\frac{\partial E}{\partial t} = \nabla^2 E - \lambda \nabla \cdot (E \nabla \alpha) + \epsilon h(x) + \frac{\gamma ET}{\eta + T} - \nu ET - \psi E, \quad (3.12a)$$

$$\frac{\partial T}{\partial t} = \phi \nabla^2 T + \beta_1 T(1 - \beta_2 T) - \mu ET, \quad (3.12b)$$

$$\frac{\partial \alpha}{\partial t} = \tau \nabla^2 \alpha + \kappa ET - \delta \alpha, \quad (3.12c)$$

where

$$\begin{aligned} \lambda &= \chi \alpha_0 t_0, & \epsilon &= \frac{st_0}{E_0}, & \gamma &= \rho t_0, & \psi &= d_1 t_0, \\ \eta &= \frac{g}{T_0}, & \nu &= l T_0 t_0, & \phi &= D_2 t_0, & \beta_1 &= a t_0, \\ \mu &= m E_0 t_0, & \tau &= D_3 t_0, & \kappa &= \frac{n E_0 T_0 t_0}{\alpha_0}, & \delta &= d_4 t_0, \quad \text{and} \quad \beta_2 = b T_0. \end{aligned}$$

The boundary and initial conditions become

$$\frac{\partial E}{\partial x}(0, t) = \frac{\partial T}{\partial x}(0, t) = \frac{\partial \alpha}{\partial x}(0, t) = 0,$$

$$\frac{\partial E}{\partial x}(1, t) = \frac{\partial T}{\partial x}(1, t) = \frac{\partial \alpha}{\partial x}(1, t) = 0,$$

$$\begin{aligned} E(x, 0) &= \begin{cases} 0, & 0 \leq x \leq L \\ [1 - \exp(-1000(x - L)^2)], & L \leq x \leq x_0, \end{cases} \\ T(x, 0) &= \begin{cases} [1 - \exp(-1000(x - L)^2)], & 0 \leq x \leq L \\ 0, & L \leq x \leq x_0, \end{cases} \\ \alpha(x, 0) &= 0, \forall x \in [0, x_0], \end{aligned}$$

respectively.

Figure 3.1 shows the initial conditions of the model (3.12) in terms of cell densities. It shows that initially, the tumour cells occupy the region  $[0, 0.2]$  while the TICLs occupy the region  $[0.2, 1]$ .

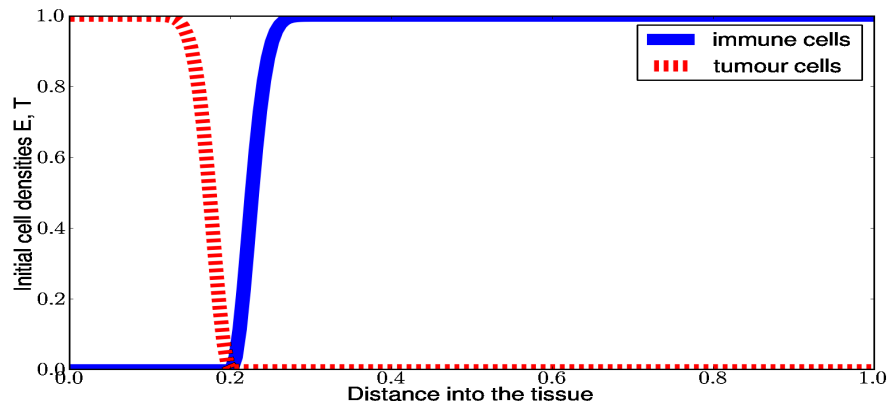


Figure 3.1: Initial cell densities of TICLs and tumour cells.

### 3.5 Numerical simulations

We use the Crank Nicholson discretization method to simulate the system (3.12). Because our system has diffusion terms, it is appropriate to use the Crank Nicholson method because it is unconditionally stable. However, due to the nature of the chemotaxis term, to prevent a blow up of our solutions, careful consideration is made when choosing the number of iterations.

The system (3.12) represents coupled non-linear PDEs, and by using the Crank Nicholson scheme, getting the next values of the solutions, for our case,  $E^{j+1}$ ,  $T^{j+1}$ , and  $\alpha^{j+1}$  in space will involve solving a system of linear algebraic equations. In cases where there are non linear terms, we discretize by considering old or previous values that are known  $(E^j, T^j, \alpha^j)$ . This will then leave the right hand side of the system (3.12) with constants.

### 3.5.1 Methodology

The Crank Nicholson method [63] transforms the components  $\frac{\partial E}{\partial t}$ ,  $\frac{\partial^2 E}{\partial x^2}$  and  $\frac{\partial E}{\partial x}$  as:

$$\frac{\partial E}{\partial t} = \frac{E_i^{j+1} - E_i^j}{\Delta t}, \quad (3.13a)$$

$$\frac{\partial^2 E}{\partial x^2} = \frac{1}{2(\Delta x)^2} \left( E_{i+1}^{j+1} - 2E_i^{j+1} + E_{i-1}^{j+1} + E_{i+1}^j - 2E_i^j + E_{i-1}^j \right), \quad (3.13b)$$

$$\frac{\partial E}{\partial x} = \frac{1}{4\Delta x} \left( E_{i+1}^{j+1} - E_{i-1}^{j+1} + E_{i+1}^j - E_{i-1}^j \right), \quad (3.13c)$$

where  $j$  and  $i$  represent position and time respectively. Applying this to equations (3.12a), (3.12b), and (3.12c) and then arranging them in such a way that the left hand side has unknown terms and the right hand has known terms, we get

$$\begin{aligned} & -(W_1 + P_1\tau_1)E_{i-1}^{j+1} + P_4E_i^{j+1} - (P_4 + W_1)E_{i+1}^{j+1} \\ & = (W_1 + P_4\tau_1)E_{i-1}^j + P_1E_i^j + \epsilon h(x) + \gamma E_i^j T_i^j \nu E_i^j T_i^j - E_i^j - P_5\tau_2 E_i^j + (P_4\tau_1 - W_1)E_{i+1}^j, \end{aligned} \quad (3.14)$$

$$\begin{aligned} -W_2T_{i-1}^{j+1} + P_2T_i^{j+1} + W_2T_{i+1}^{j+1} & = -W_2T_{i+1}^j + P_2T_i^j + \beta_1T_i^j - \beta_1\beta_2T_i^jT_i^j - \mu E_i^jT_i^j - W_2T_{i-1}^j, \end{aligned} \quad (3.15)$$

$$\begin{aligned} -W_3\alpha_{i-1}^{j+1} + P_3\alpha_i^{j+1} + W_3\alpha_{i+1}^{j+1} & = -W_2\alpha_{i+1}^j + P_3\alpha_i^j + \beta_1T_i^j - \kappa E_i^jT_i^j - \delta\alpha_i^j - W - 3\alpha_{i+1}^j, \end{aligned} \quad (3.16)$$

where

$$\begin{aligned} \tau_1 & = \alpha_{i+1}^{j+1} - \alpha_{i-1}^{j+1} + \alpha_{i+1}^j - \alpha_{i-1}^j, \\ \tau_2 & = \alpha_{i+1}^{j+1} - 2\alpha_i^{j+1} + \alpha_{i-1}^{j+1} + \alpha_{i+1}^j - 2\alpha_i^j + \alpha_{i-1}^j. \end{aligned}$$

Using the boundary conditions 3.8, together with forward finite differences, the first and last terms become;

$$E_1^j = E_0^j, \quad T_1^j = T_0^j, \quad \text{and,} \quad \alpha_1^j = \alpha_0^j \quad \text{for any } j,$$

$$E_{N+1}^j = E_{N-1}^j, \quad T_{N+1}^j = T_{N-1}^j, \quad \text{and} \quad \alpha_{N+1}^j = \alpha_{N-1}^j \quad \text{for any } j.$$

We solve (3.14), (3.15), and (3.16) simultaneously by arranging the left hand sides into matrices and solving first for  $\alpha$  and  $T$  before  $E$  is found. The left hand tridiagonal matrices for the three equations are:

$$A_E = \begin{pmatrix} -\chi_1 & (P_4 - W_1) & 0 & \cdots & \cdots & 0 \\ P_1\tau_1 - W_1 & P_1 & P_4 - W_1 & 0 & 0 & \vdots \\ 0 & P_1\tau_1 - W_1 & P_1 & P_4 - W_1 & 0 & \vdots \\ \vdots & \vdots & \vdots & \vdots & 0 & \vdots \\ \vdots & 0 & 0 & P_1\tau_1 - W_1 & P_1 & P_4 - W_1 \\ 0 & 0 & 0 & 0 & \chi_2 & P_1 \end{pmatrix} \begin{pmatrix} E_1^{j+1} \\ E_2^{j+1} \\ \vdots \\ \vdots \\ E_{N-1}^{j+1} \\ E_N^{j+1} \end{pmatrix},$$

$$A_T = \begin{pmatrix} P_2 - W_2 & -W_2 & 0 & \cdots & \cdots & 0 \\ -W_2 & P_2 & -W_2 & 0 & 0 & \vdots \\ 0 & -W_2 & P_2 & -W_2 & 0 & \vdots \\ \vdots & \vdots & \vdots & \vdots & 0 & \vdots \\ \vdots & 0 & 0 & -W_2 & P_2 & -W_2 \\ 0 & 0 & 0 & 0 & -2W_2 & P_2 \end{pmatrix} \begin{pmatrix} T_1^{j+1} \\ T_2^{j+1} \\ \vdots \\ \vdots \\ T_{N-1}^{j+1} \\ T_N^{j+1} \end{pmatrix},$$

and

$$A_\alpha = \begin{pmatrix} P_3 - W_3 & -W_3 & 0 & \cdots & \cdots & 0 \\ -W_3 & P_3 & -W_3 & 0 & 0 & \vdots \\ 0 & -W_3 & P_3 & -W_3 & 0 & \vdots \\ \vdots & \vdots & \vdots & \vdots & 0 & \\ \vdots & 0 & 0 & -W_3 & P_3 & -W_3 \\ 0 & 0 & 0 & 0 & -2W_3 & P_3 \end{pmatrix} \begin{pmatrix} \alpha_1^{j+1} \\ \alpha_2^{j+1} \\ \vdots \\ \vdots \\ \alpha_{N-1}^{j+1} \\ \alpha_N^{j+1} \end{pmatrix},$$

respectively, where

$$\chi_1 = (W_1 + P_1\tau_1 - P_1), \quad \chi_2 = -2W_1 + P_1 - \tau_1 P_1$$

and the right hand sides (known values) correspond to

$$\begin{aligned} bE &= (W_1 + P_4\tau_1)E_{i-1}^j + P_1E_i^j + \epsilon h(x) + \gamma E_i^j T_i^j \nu E_i^j T_i^j - E_i^j - P_5\tau_2 E_i^j + (P_4\tau_1 - W_1)E_{i+1}^j, \\ bT &= -W_2T_{i+1}^j + P_2T_i^j + \beta_1T_i^j - \beta_1\beta_2T_i^jT_i^j - \mu E_i^jT_i^j - W_2T_{i-1}^j, \\ b\alpha &= -W_2\alpha_{i+1}^j + P_3\alpha_i^j + \beta_1T_i^j - \kappa E_i^jT_i^j - \delta\alpha_i^j - W - 3\alpha_{i+1}^j, \end{aligned}$$

where

$$\begin{aligned} W_1 &= \frac{1}{2h^2}, \quad W_2 = \frac{\phi}{2h^2}, \quad \text{and} \quad W_3 = \frac{\tau}{2h^2}, \\ P_1 &= \frac{2W_1dt + 1}{dt}, \quad P_2 = \frac{2W_2dt + 1}{dt}, \quad \text{and} \quad P_3 = \frac{2W_3dt + 1}{dt}, \end{aligned}$$

and

$$dt = \text{time step}, \quad \text{and} \quad h = \text{space step}.$$

The parameter values used are from Matzavinos et al. [6]. They however correspond to in vitro settings because in vivo measurements in literature are insufficient. We used Gaussian elimination to solve the individual systems of equations and implemented it in *PYTHON* programming software to solve for  $E$ ,  $T$ , and  $\alpha$  for each time step.

### 3.5.2 Numerical simulation results

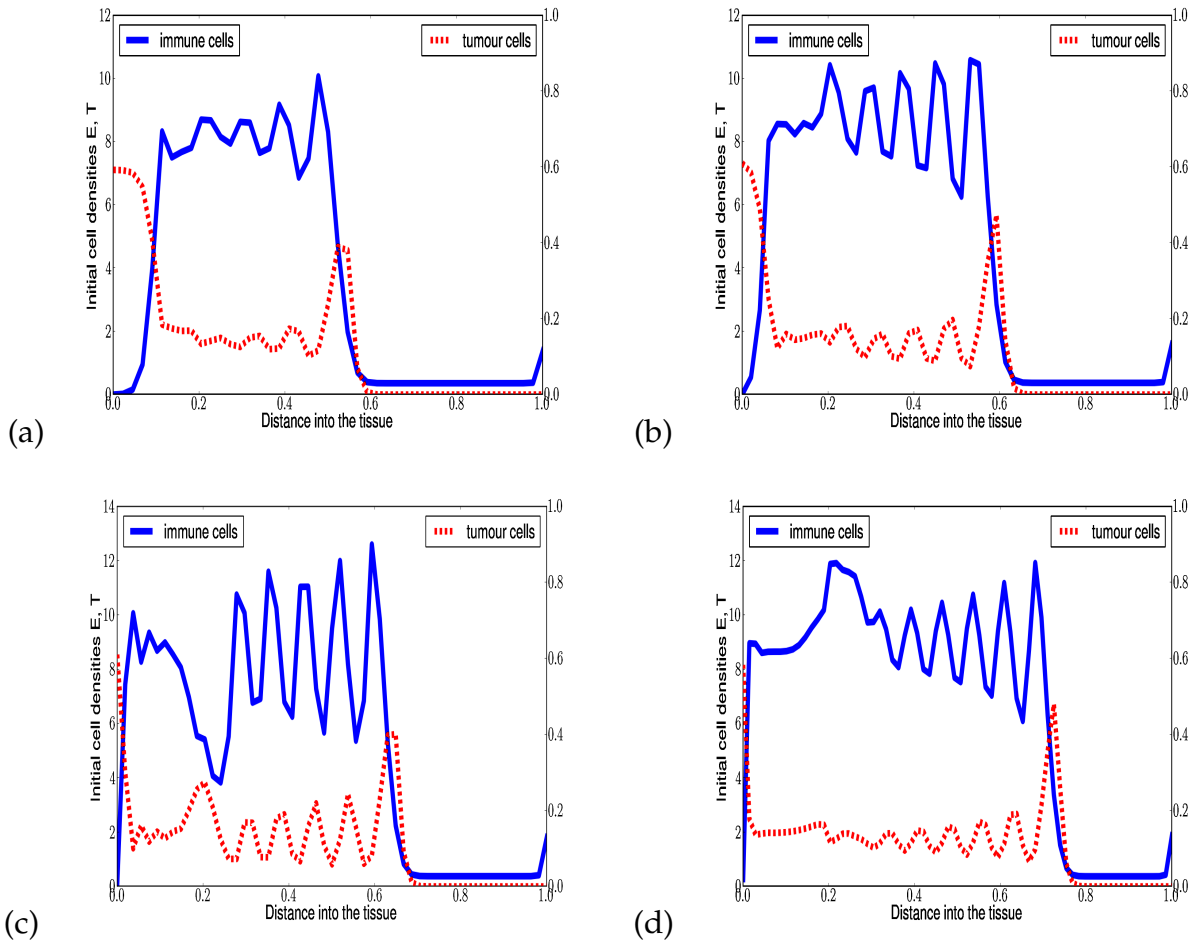


Figure 3.2: Spatial distribution of immune (TICLs) and tumour cell densities in the tissue at times corresponding to (a) 600, (b) 700, (c) 800 and (d) 1000 days respectively. The left and right hand scales correspond to TICLs and tumour cell densities respectively.

The model (3.12) was simulated using parameter values in Tables 2.3 and 3.1. Figures 3.2(a)-(d) show the spatial distribution dynamics of TICLS and tumour cell densities in the tissue at times corresponding to 100, 700, 800 and 1000 days respectively. The graphs show that the TICL density remains dominant in the

tissue. Furthermore, they show that with time, TICLs manage to bring down the tumour density to a dormant state. Initially (see Figure 3.1), the tumour cells are concentrated on one side of the domain ( $[0,0.2]$ ) and the immune cells on another ( $[0.2,1]$ ). The tumour cells invade the tissue with a soliton-like wave but are subsequently reduced by the TICLs.

In Figure 3.2, we set two scales on either sides using *twinx* in *PYTHON* software, to clearly distinguish the tumour and immune cell dynamics. The right hand scale, from 0.0 to 1.0 corresponds to the tumour cell density while that on the left from 0.0 to 12.0 and 16.0 corresponds to TICLs cell density.

### 3.6 Travelling wave simulation and analysis

A travelling wave is a one in which the medium moves in the direction of propagation of the wave. Travelling wave analysis is of great importance in our model because, if travelling waves exist, then the tumour invades the healthy tissue at its full potential [62]. If this happens, we would expect that with time the immune cells are highly probable to outweigh the tumour cell density. In this section, we investigate the existence of travelling wave solutions that emerge as a result of a certain range of values of  $\mu$ ,  $\beta_1$  and  $\epsilon$ . For simplicity, we ignore the effects of chemotaxis [62]. This simplifying assumption is reasonable because according to Matzavinos et al. [64], the propagation of travelling waves is not influenced by chemotaxis. Further more, we set the Heaviside function  $h(x)$  to 1. We thus, consider the non dimensionalised system below:

$$\frac{\partial E}{\partial t} = \nabla^2 E + \epsilon + \frac{\gamma ET}{\eta + T} - \nu ET - \psi E, \quad (3.17a)$$

$$\frac{\partial T}{\partial t} = \phi \nabla^2 T + \beta_1 T(1 - \beta_2 T) - \mu ET. \quad (3.17b)$$

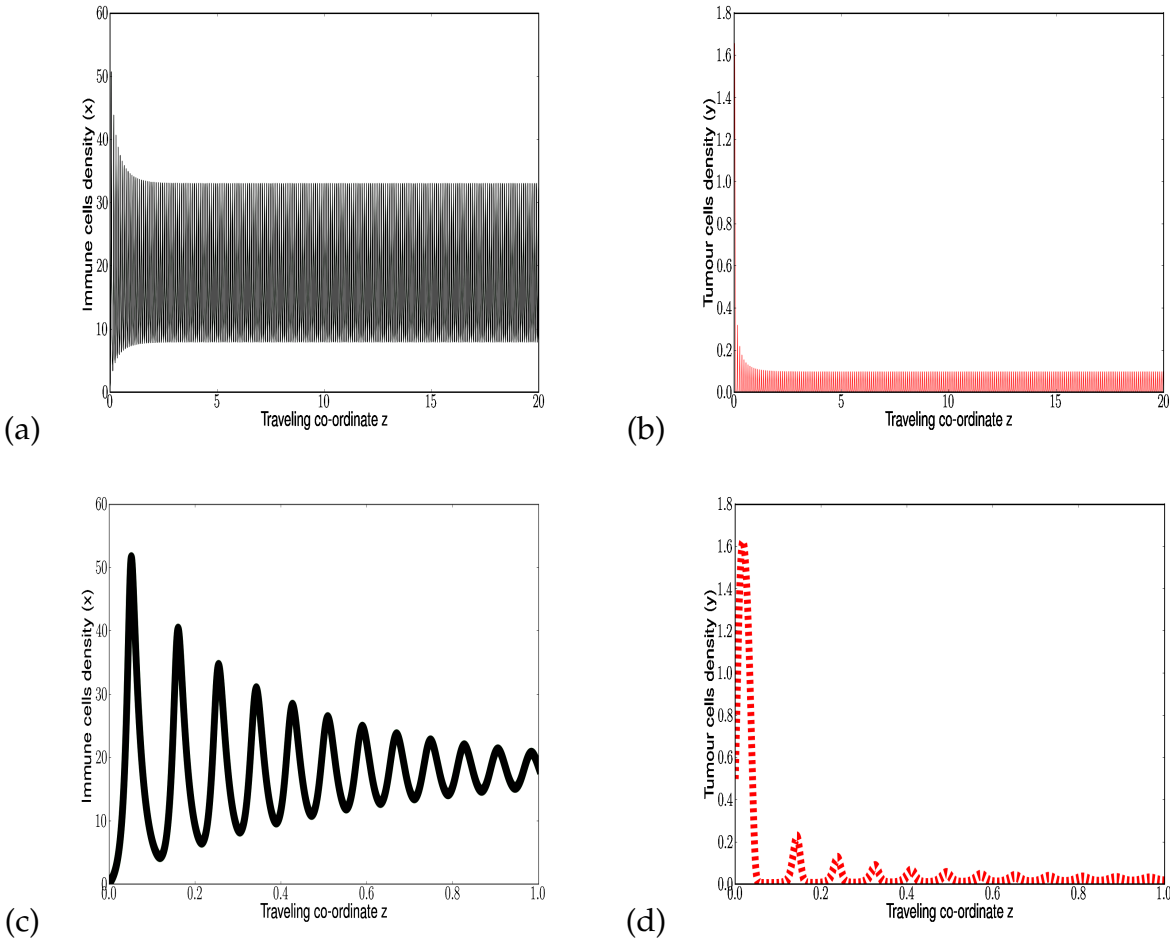


Figure 3.3: Travelling wave solutions of the system (3.18) for a long (a,b) and short time periods (c,d).

The numerical simulations (see Figure 3.3(a)-(d)) indicate that the system of equations exhibits travelling wave solutions for some choice of parameters. We use the geometric treatment of an apt phase space with the aim of establishing the intersection between a stable and unstable manifolds [62]. We specify a travelling

co-ordinate  $z = x + ct$  where  $c > 0$  and let  $\tilde{E}(z) = E(x, t)$ , and  $\tilde{T}(z) = T(x, t)$ . It is worth noting that the travelling co-ordinate above is different from that considered by Bellomo et al. [62]. Our travelling waves are from the right to the left. By using the chain rule and a change of variables,

$$\frac{\partial \tilde{E}}{\partial t} = \frac{d\tilde{E}}{dz} \cdot \frac{\partial z}{\partial t}, \quad \text{and} \quad \frac{\partial \tilde{T}}{\partial t} = \frac{d\tilde{T}}{dz} \cdot \frac{\partial z}{\partial t}.$$

the system (3.17) without the tildes, becomes

$$c \frac{dE}{dz} = \frac{d^2E}{dz^2} + \epsilon + \frac{\gamma ET}{\eta + T} - \nu ET - \psi E, \quad (3.18a)$$

$$c \frac{dT}{dz} = \phi \frac{d^2T}{dz^2} + \beta_1 T(1 - \beta_2 T) - \mu ET. \quad (3.18b)$$

Our intention is to take advantage of phase space techniques and thus we formulate the system (3.18) in  $\mathbb{R}^4$ . In particular we define new variables

$$E_1 = \frac{dE}{dz}, \quad \text{and} \quad T_1 = \frac{dT}{dz}.$$

The system can therefore be transformed as

$$\frac{dx}{dz} = f(x) \quad \text{where} \quad \left( \begin{array}{c} E_1 \\ E \\ T_1 \\ T \end{array} \right) \in \mathbb{R}^4, \quad (3.19)$$

and

$$f(x) = \left[ \begin{array}{c} -cE_1 - \epsilon - \frac{\gamma ET}{(\eta+T)} + \nu ET + \psi E \\ E_1 \\ -c\frac{T_1}{\phi} - \frac{\beta_1}{\phi} T(1 - \beta_2 T) + \frac{\mu ET}{\phi} \\ T_1 \end{array} \right]. \quad (3.20)$$

The system (3.19) can be regarded as an eigenvalue problem because the wave velocity,  $c$  is unknown. Several analytical methods have been developed for estimating  $c$  but for our case, we take  $c \approx 850$ , as used by Bellomo et al. [62]. The idea behind travelling wave analysis is to find a heteroclinic connection between  $X^0$  and  $X^1$  where

$$X^0 \approx \begin{pmatrix} 0 \\ 0.546 \\ 0 \\ 0.305 \end{pmatrix} \quad \text{and} \quad X^1 \approx \begin{pmatrix} 0 \\ 0.3301 \\ 0 \\ 0 \end{pmatrix}. \quad (3.21)$$

Here  $X^0$  and  $X^1$  are steady state solutions to the system (3.18) obtained by equating equations (3.18a) and (3.18b) to zero. Our interest is to establish the existence of an orbit  $X_{con}(z)$  that satisfies

$$\lim_{z \rightarrow -\infty} X_{con}(z) = X^0 \quad \text{and} \quad \lim_{z \rightarrow \infty} X_{con}(z) = X^1. \quad (3.22)$$

The existence of such an orbit would imply that travelling wave solutions do exist [62]. We consider the linearisation

$$\frac{dX}{dz} = Df(X^0)x, \quad \text{and} \quad \frac{dX}{dz} = Df(X^1)X \quad (3.23)$$

of the vector field  $f$  at the equilibrium points  $X^0$  and  $X^1$  respectively. From the Jacobian

$$J(x) = \begin{pmatrix} -c & \frac{-\gamma T}{(\eta+T)} + \nu E + \psi & 0 & \frac{-\eta\gamma E}{(\eta+T)^2} \\ 1 & 0 & 0 & 0 \\ 0 & 0 & \frac{-C}{\phi} & \frac{\beta_1}{\phi} + \frac{2\beta_1\beta_2}{\phi} + \frac{\mu E}{\phi} \\ 0 & 0 & 1 & 0 \end{pmatrix} \quad (3.24)$$

of the system (3.20), we determine the spectrum of the matrices  $Df(X^0)$  and  $Df(X^1)$ . For values of the parameters for the system (3.20) under discussion,  $Df(X^0)$  has four real eigenvalues, two positive and two negative. The eigenvalues imply the existence of a 2-dimensional stable manifold  $W^s(X^1)$ . Similarly,  $Df(X^1)$  has four eigenvalues, one positive and three negative, implying the existence of an unstable 3-dimensional manifold  $W^u(X^0)$ . From this result, we note that

$$\dim(W^u(X^0)) + \dim(W^s(X^1)) = \dim\mathbb{R}^4 + 1 \quad (3.25)$$

Equation (3.25) suggests that  $W^u(X^0)$  and  $W^s(X^1)$  probably intersect transversally along a one-dimensional curve in the four-dimensional phase space. This is because the solutions of the system (3.20) lie in four dimension (4D) but the summation of the dimension of the stable and unstable manifolds is five (5D) just as shown in equation (3.25) (see [30, 62]). If this is the case, then this curve would define a generic heteroclinic connection [62]. The simulations of (3.20) portray travelling wave solutions (shown in Figure 3.3) that maintain their structure with time.

We in this Chapter presented a mathematical model of tumour-TICLs interactions which incorporated local interaction kinetics, the diffusion of TICLs and tumour cells, and the chemotactic movement of the TICLs towards the tumour. In Section 3.5, We used the Crank Nicholson scheme to simulate the resulting system of PDEs. Furthermore, We in Section 3.6, performed a travelling wave analysis and discussed the implications of such solutions. Finally, we explained the possible implications of the results. We discovered from the numerical simulations that the TICLs bring down the tumour density to some dormant state and that the TICLs reduce the tumour cell concentration through out the tissue. In the next Chapter we develop two new models that incorporate immunotherapy and we investigate

its effects on the tumour-TICLs interactions that we have already discovered in Chapters 2 and 3.

## Chapter 4

# TICLs-tumour cell interaction with immunotherapy

In Chapter 2 we investigated the TICLs-tumour interaction without any form of treatment and found that while TICLs alone are not enough to completely eradicate tumour cells in the body, they bring a tumour to a dormant and a lower stable state (cancer dormant state). In this Chapter we start by developing a model that includes immunotherapy. We find the steady state solutions for this model and investigate their stability. As in the previous homogeneous model, we also analyse the model's phase space and perform numerical simulations with well defined parameter values. Then, we consider spatial distribution, by formulating a suitable model and numerically analysing its spatial-temporal dynamics. Finally, we give possible insights as to the application and reliability of the results.

We focus on immunotherapy as a stimulus to the immune system. We therefore assume that there is no cell complex formation as a result of  $IL_2$  binding to the immune cells. Specifically, We consider the case of immunotherapy employing

cytokines in adaptive cellular immunotherapy (ACI); the main cytokine responsible for lymphocyte activation, growth and differentiation being  $IL_2$  (see Section 1.2).

## 4.1 Model development

In this section, we develop a model to study the tumour-TICLs interaction with immunotherapy. The model considers local kinetic interactions as described in Chapter 2 in addition to the effects of  $IL_2$ . It subdivides the cell population into local densities of hunting TICLs  $E$ , tumour cells  $T$ , tumour-TICLs complex concentration  $C$ , Interleukine2 concentration  $IL_2$ , and a resting TICLs  $R$ . In addition to the  $IL_2$  class introduced, we in this model consider a new class of resting TICLs. We assume that these are cells from which the hunting TICLs are recruited (see models in [65, 66]). As described in Section 1.2), we assume that with immunotherapy there is an interaction of cultured immune cells ( $IL_2$ ) that have anti tumour reactivity with the tumour host. We assume that  $IL_2$  does not necessarily bind with TICLs to form a cell complex but rather stimulates the TICLs to fight cancer through lymphocyte activation, growth and differentiation. We also assume that  $IL_2$  increases the rate of conversion of resting TICLs to hunting TICLs (see [66]).

Table 4.1: **State variables for the tumour-immune cells model with immunotherapy (4.1).**

State variable	Description
$E$	Concentration of activated TICLs in cells per centimetre.
$T$	Concentration of tumour cells in cells per centimetre.
$C$	Concentration of tumour-TICLs cell complexes in cells per centimetre.
$IL_2$	Interluikine concentration in U per $m^2$ .
$R$	Resting TICLs in cells per centimetre.

With the above assumptions, we get a system of five coupled non-linear ODEs.

$$\frac{dE}{dt} = \rho R + \frac{fC}{g_1 + T} - d_1 E - k_1 ET + (k_{-1} + k_2 p)C + \omega IL_2 R + \frac{\theta_2 E IL_2}{g_2 + IL_2} + cT, \quad (4.1a)$$

$$\frac{dT}{dt} = a_1 T(1 - b_1 T) - k_1 ET + (k_{-1} + k_2(1 - p))C, \quad (4.1b)$$

$$\frac{dC}{dt} = k_1 ET - (k_{-1} + k_2)C, \quad (4.1c)$$

$$\frac{dIL_2}{dt} = s_2 + \frac{\theta_3 ET}{g_3 + T} - d_2 IL_2, \quad (4.1d)$$

$$\frac{dR}{dt} = s_3 + a_2 R(1 - b_2 R) - \omega IL_2 R - \rho R, \quad (4.1e)$$

where  $\theta_2 E IL_2 / (g_2 + IL_2)$  is a proliferation term also considered by Kirschener and Panetta [32]. It is a term that models the stimulation of TICLs by  $IL_2$  and is of the Michaelis-Menten form [32].  $\theta_2$  and  $g_2$  are Michaelis-Menten constants, obtained from experimental results. The term  $\theta_3 ET / (g_3 + T)$  is also a proliferation term that is as a result of tumour-TICLs interactions. It is also of Michaelis-Menten form and it is used to account for the self-limiting production of  $IL_2$ .  $\theta_3$  and  $g_3$  are also Michaelis-Menten constants. Just like in Chapter 2, the TICLs cells proliferation term is considered to be  $fC / (g + T)$ .

Table 4.2: Newly introduced Parameter description for the tumour-immune cells interaction model with immunotherapy (4.1).

Parameter	Description
$s_2$	Rate of $IL_2$ is supply (amount of $IL_2$ injected into the tissue).
$s_3$	Rate of resting TICLs supply.
$\omega$	Stimulation rate of resting TICLs to hunting cells as a result of $IL_2$ supply.
$\rho$	Recruitment rate of hunting TICLs from the resting cells.
$c$	Ability of $IL_2$ to provoke an immune response (antigenicity rate).
$a_2$	Growth rate of resting TICLs.
$b_2$	inverse of carrying capacity for resting TICLs.
$d_2$	Rate of decay of $IL_2$ .

As in Chapters 2 and 3, we assume that formation of cellular conjugates occurs on a time scale of a few minutes, that is  $dC/dt \approx 0$ . The system (4.1) then reduces to a system of four coupled non-linear ODEs,

$$\frac{dE}{dt} = \rho R + \frac{\theta_1 ET}{g_1 + T} - d_1 E - l ET + \omega IL_2 R + \frac{\theta_2 E IL_2}{g_2 + IL_2} + c T, \quad (4.2a)$$

$$\frac{dT}{dt} = a_1 T(1 - b_1 T) - m ET, \quad (4.2b)$$

$$\frac{dIL_2}{dt} = s_2 + \frac{\theta_3 ET}{g_3 + T} - d_2 IL_2, \quad (4.2c)$$

$$\frac{dR}{dt} = s_3 + a_2 R(1 - b_2 R) - \omega IL_2 R - \rho R, \quad (4.2d)$$

where

$$l = Kk_2(1 - p), \quad \theta_1 = fK, \quad \text{and} \quad m = Kk_2p.$$

## 4.2 Non-dimensionalization

We begin the analysis of the model (4.2) by non-dimensionalizing the system of equations by scaling the concentrations of  $E$ ,  $T$ ,  $IL_2$  and  $R$  as;

$$x = \frac{E}{E_0}, \quad y = \frac{T}{T_0}, \quad z = \frac{IL_2}{IL_{20}}, \quad w = \frac{R}{R_0}, \quad \text{and} \quad \bar{t} = \frac{t}{t_0}. \quad (4.3)$$

The order of magnitude of the concentrations for TICLs and tumour cells are the same as in Chapter 2 (i.e  $E_0 = 10^6$  cells/cm and  $T_0 = 10^7$ ) cells/cm, we also set  $R_0 = 10^7$  cells/cm.  $IL_{20}$  is set to be  $10^9$  cells/cm, a value that also lies in the range of concentrations or dosage that a human body can contain [67]. Time is scaled relative to the rate of TICLs' deactivation, i.e  $t_0 = d_1^{-1}$ . This gives a four-dimensional system of fractional populations  $x$ ,  $y$ ,  $z$ , and  $w$ . We drop the bar on the non-dimensionalised time  $\bar{t}$  for convenience. The model (4.2) can then be re-expressed as:

$$\frac{dx}{dt} = \bar{\phi}_1 w + \frac{\bar{\theta}_1 xy}{\eta_1 + y} - \nu xy - x + \frac{\bar{\theta}_2 xz}{\eta_2 + z} + \bar{\omega}_1 wz + \bar{c}y, \quad (4.4a)$$

$$\frac{dy}{dt} = \beta_1 y(1 - \beta_2 y) - \bar{\mu}_1 xy, \quad (4.4b)$$

$$\frac{dz}{dt} = \sigma_2 + \frac{\bar{\theta}_3 xy}{\eta_3 + y} - \bar{\mu}_2 z, \quad (4.4c)$$

$$\frac{dw}{dt} = \sigma_3 + \alpha_1 w(1 - \alpha_2 w) - \bar{\omega}_2 wz - \bar{\phi}_2 w, \quad (4.4d)$$

where

$$\bar{\phi}_1 = \frac{\rho R_0}{E_0 d_1}, \quad \bar{\theta}_1 = \frac{\theta_1}{d_1}, \quad \eta_1 = \frac{g_1}{T_0}, \quad \nu = \frac{l T_0}{d_1}, \quad \bar{c} = \frac{c T_0}{E_0 d_1},$$

$$\bar{\omega}_1 = \frac{\omega_1 R_0 IL_{20}}{E_0 d_1}, \quad \beta_1 = \frac{a}{d_1}, \quad \beta_2 = b T_0, \quad \bar{\mu}_1 = \frac{m E_0}{d_1}, \quad \sigma_3 = \frac{s_3}{R_0 d_1},$$

$$\bar{\theta}_2 = \frac{\theta_1}{d_1}, \quad \eta_2 = \frac{g_2}{IL_{20}}, \quad \bar{\omega}_2 = \frac{\omega IL_{20}}{d_1}, \quad \sigma_2 = \frac{s_2}{E_0 d_1}, \quad \bar{\phi}_2 = \frac{\rho}{d_1},$$

$$\bar{\theta}_3 = \frac{\theta_3}{d_1}, \quad \eta_3 = \frac{g_3}{d_1}, \quad \bar{\mu}_2 = \frac{\mu_2}{d}, \quad \alpha_1 = \frac{a_2}{d_1}, \quad \text{and} \quad \alpha_2 = b_2 R_0.$$

In the above system of equations (4.4),  $x$ ,  $y$ ,  $z$  and  $w$  carry no physical meaning when  $x < 0$ ,  $y < 0$ ,  $z < 0$  and  $w < 0$ . For this model, there exists a domain  $\mathbb{D}$  in which the system of equations is mathematically and epidemiologically well-defined. We define this domain  $\mathbb{D}$  as

$$\mathbb{D} = \left\{ \left( \begin{array}{c} x \\ y \\ z \\ w \end{array} \right) \in \mathbb{R}^4 \left| \begin{array}{l} x \geq 0 \\ y \geq 0 \\ z \geq 0 \\ w \geq 0 \end{array} \right. \right\}.$$

### 4.3 Steady state solutions and stability analysis

Finding analytical solutions to model (4.4) is a difficult undertaking because the system is coupled and non-linear. We therefore in this section investigate the long term behaviour of the solutions by calculating the system's steady state solutions. We get the steady state solutions by equating the system of equations (4.4) to zero. Using the parameter values given in Tables 2.3 and 4.3 together with  $g_3 = 10^3 \text{ cm}^3$ , a value lower than that in Kirschener and Panetta [32] and  $s_2 = 7.9 \times 10^7 \text{ U/m}^2$ , a value that we choose motivated by the study on dosages of  $IL_2$  in Tritarelli et al. [67], we obtain seven steady state solutions, one healthy steady state (TFE), a steady state depicting cancer dormancy and five solutions that are biologically meaningless because they do not lie in the domain  $\mathbb{D}$ . Of these five, two are

complex and three have some negative solutions. The two feasible steady states (healthy and cancer dormant states) are;

$$E_1 = (x_1, y_1, z_1, w_1) = (0.3301, 0, 0.796, 0.001),$$

$$E_2 = (x_2, y_2, z_2, w_2) \approx (5.89, 0.798, 0.82, 0.00016).$$

To investigate the stability of the steady states above, we linearise the system (4.4) about each of the steady states to obtain

$$\frac{dX_i}{dt} = A_i X_i,$$

where  $A_i$  is the Jacobian matrix of the system evaluated at the steady state.

For  $i = 1$ , there are four eigenvalues  $\lambda_1 = -1$ ,  $\lambda_2 = -242$ ,  $\lambda_3 = -192.6$  and  $\lambda_4 = 3.94$ , that is three negative and one positive, implying that  $(x_1, y_1, z_1, w_1)$  representing a healthy steady state is unstable. For  $i = 2$ , there are four complex eigenvalues  $\lambda_{1,2} = -0.3 \pm 5.16i$  and  $\lambda_3 = -242.018 \pm 5.16i$  with negative real parts, implying that  $(x_2, y_2, z_2, w_2)$  representing a tumour dormant steady state is a stable focus. This tumour dormant steady state suggests that immunotherapy does not completely eliminate tumour cells from the human body but rather brings the tumour cell concentration to a lower cancer dormant state.

## 4.4 Phase space analysis

Using the parameter values in Tables 2.3, and 4.3, we plot the phase portrait of  $y$  the fractional tumour density against  $x$ , the fractional TICLs cell density in Figure 4.1.

Table 4.3: **Dimensional parameter values obtained from Kirschener and Panetta [32] and Borges et al. [66].**

Parameter	Estimated value	Units
$\theta_2$	0.1245	day <sup>-1</sup>
$\theta_3$	5	day <sup>-1</sup>
$c$	$0 \leq c \leq 0.005$	day <sup>-1</sup>
$g_2$	$10^7$	cm <sup>3</sup>
$d_2$	10	day <sup>-1</sup>
$a_2$	0.0245	day <sup>-1</sup>
$b_2$	$10^{-7}$	cell <sup>-1</sup>
$\rho$	$6.2 \times 10^{-9}$	cells <sup>-1</sup> day <sup>-1</sup>

As can be seen from Figure 4.1, the phase space of the fractional densities of TICLs and tumour cells respectively spiral to a stable focus (tumour dormant state). The spiralling occurs at a fast rate due to the introduction of immunotherapy. We have shown that the solutions to the system (4.4) spiral to a cancer dormant state. We proceed to show using the Dulac-Bendixon theorem [55] that model (4.4) has no closed orbits in  $\mathbb{D}$ . This will help us in determining whether the system (4.4) has periodic solutions or not.

**Theorem 4.1** *The system (4.4) has no closed orbits for positive values of  $x$ ,  $y$ ,  $z$  and  $w$ .*

*Proof*

In a similar way to that did with system (2.5) (see Theorem 2.4 in Chapter 2), using Dulac's criterion, it is equivalent to show that

$$\frac{\partial}{\partial x} (\phi(x, y, z, w)\dot{x}) + \frac{\partial}{\partial y} (\phi(x, y, z, w)\dot{y}) + \frac{\partial}{\partial z} (\phi(x, y, z, w)\dot{z}) + \frac{\partial}{\partial w} (\phi(x, y, z, w)\dot{w}) \neq 0$$

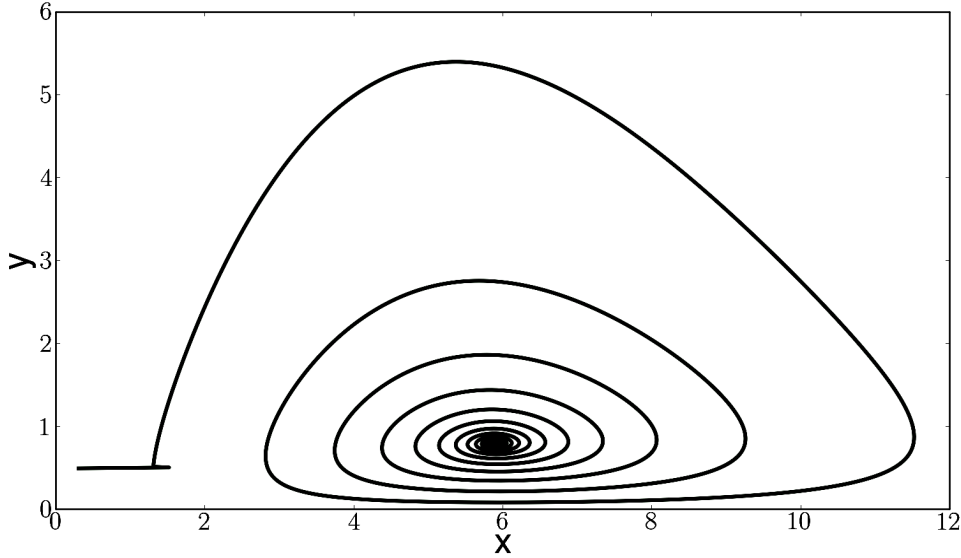


Figure 4.1: Orbit of the ODE system (4.2) converging to the tumour dormant state.

$\forall x, y, z, w \in \mathbb{D}$ .

Consider

$$\phi(x, y, z, w) = \frac{1}{xyzw},$$

$$\begin{aligned} \nabla \cdot (g\dot{X}) &= \frac{\partial}{\partial x} (\phi(x, y, z, w)\dot{x}) + \frac{\partial}{\partial y} (\phi(x, y, z, w)\dot{y}) + \frac{\partial}{\partial z} (\phi(x, y, z, w)\dot{z}) + \frac{\partial}{\partial w} (\phi(x, y, z, w)\dot{w}), \\ &= -\frac{\bar{\theta}_1}{x^2yz} - \frac{\omega_1}{x^2y} - \frac{\bar{c}}{x^2zw} - \frac{\beta_1\beta_2}{xzw} - \frac{\sigma_2}{xyz^2w} - \frac{\bar{\theta}_3}{z^2w(\eta_3 + y)} - \frac{\sigma_3}{xyzw^2} - \frac{\alpha_1\alpha_2}{xyz}, \\ &= -\left( \frac{\bar{\theta}_1}{x^2yz} + \frac{\omega_1}{x^2y} - \frac{\bar{c}}{x^2zw} + \frac{\beta_1\beta_2}{xzw} + \frac{\sigma_2}{xyz^2w} + \frac{\bar{\theta}_3}{z^2w(\eta_3 + y)} + \frac{\sigma_3}{xyzw^2} + \frac{\alpha_1\alpha_2}{xyz} \right). \end{aligned}$$

Since we assumed that all parameter values are positive, it implies that

$\nabla \cdot (g\dot{X}) < 0 \forall x, y, z, w \in \mathbb{D}$ , where

$$\mathbb{D} = \left\{ \left( \begin{array}{c} x \\ y \\ z \\ w \end{array} \right) \in \mathbb{R}^4 \mid \begin{array}{l} x \geq 0 \\ y \geq 0 \\ z \geq 0 \\ w \geq 0 \end{array} \right\}.$$

■

We have shown that the system (4.4) has no periodic solutions thereby ruling out the possibility of regularly repeating processes. We next simulate the model (4.4) to determine its numerical solutions since the analytical solutions are hard to get.

## 4.5 Numerical simulations of the model

Using the parameter values in Tables 2.3, and 4.3, together with  $g_3 = 10^3 \text{ cm}^3$ , a value lower than that in Kirschener and Panetta [32] and  $s_2 = 7.9 \times 10^7 \text{ U/m}^2$ , a value that we choose motivated by the study on dosages of  $IL_2$  in Tritarelli et al. [67]. The results are shown in figures 4.2 and 4.3.

From Figure 4.2, it can be seen that the tumour cell concentration reduced from 0.919 in approximately six years, with the case without immunotherapy (see Section 2.5, Figure 2.5) to 0.796 in approximately three years. This is a much shorter time than the time for a similar outcome shown in Figure 2.5). Thus due to the introduction of immunotherapy to the system, tumour cell concentration is lowered down to a dormant state, which is stable in a much shorter time than with no immunotherapy.

Similarly Figure 4.3 which shows the variation of TICLs cell and tumour cell densities with immunotherapy, against time on different concentration scales, may be

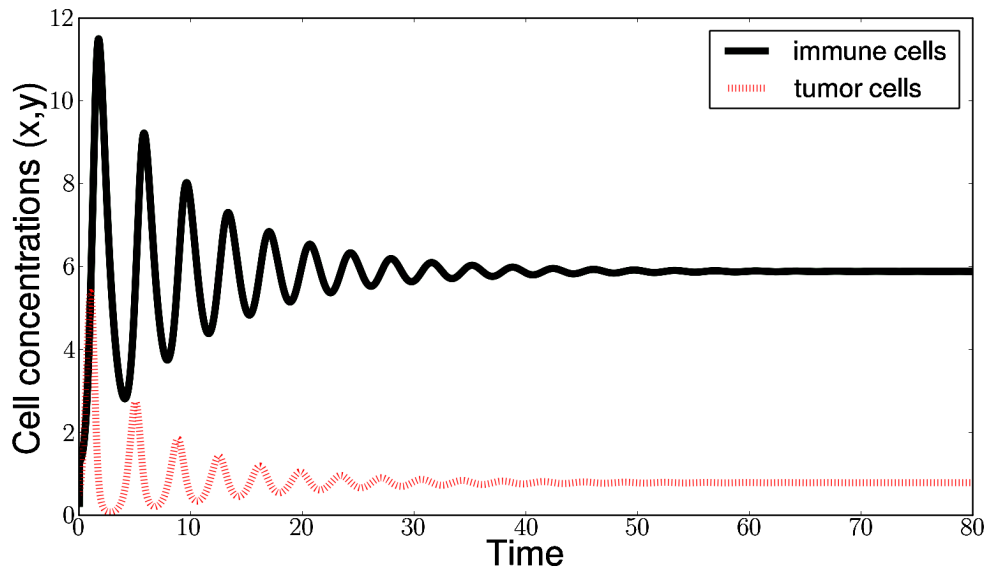


Figure 4.2: Plots of cell densities with immunotherapy against non-dimensional time.

compared with Figure 2.6 (with no immunotherapy). In all the numerical simulations, we considered the initial conditions to be  $x(0) = 0.3$ ,  $y(0) = 0.5$ ,  $z(0) = 1$ , and  $w(0) = 0.1$  and we used Eulers numerical scheme with  $n$ , the number of iterations equal to 20,000. This was implemented in *PYTHON*. From the numerical solutions of the model (4.2) one can then conclude that immunotherapy aids in bringing the tumour cells to a dormant state but can not completely aid TICLs in eradicating them.

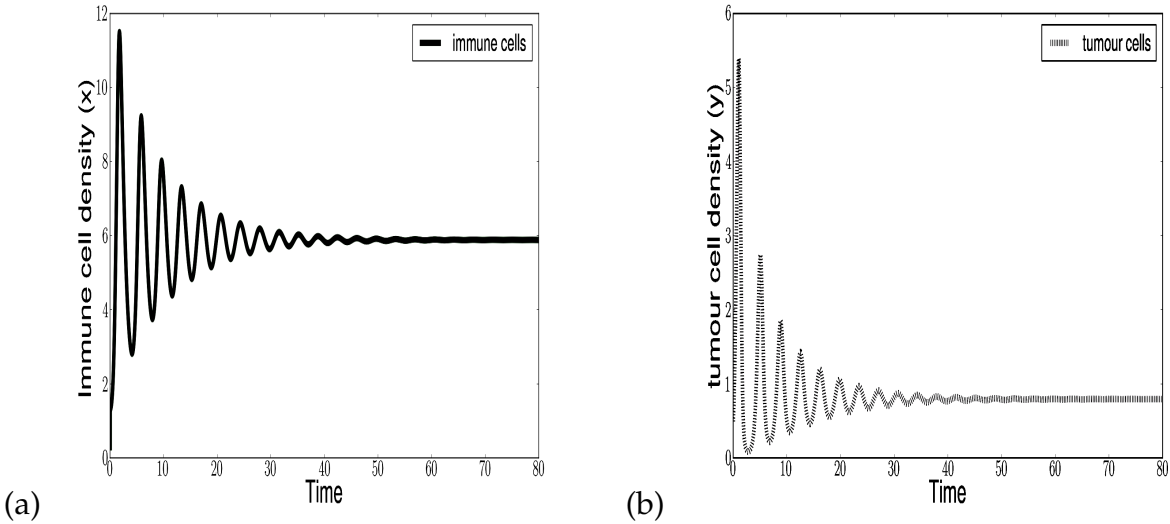


Figure 4.3: Variation of immune (TICLs) and tumour cell densities with immunotherapy against time. The time is non-dimensional

## 4.6 Immunotherapy model in a spatially heterogeneous domain

In this section we consider the spatial distribution of the TICLs, resting TICLs, tumour cells, and  $IL_2$ . We do this to compare and contrast the effects of immunotherapy on TICLs-tumour interactions with the incorporation of space.

### 4.6.1 Model development

We assume that  $IL_2$  diffuses in the body. This is a reasonable assumption because it is a protein like substance and indeed its mechanism of movement in the body is through diffusion (see Cornelissen et al. [68]). We maintain the same elements considered in (3.7), that is, chemotaxis and diffusion for the TICLs and diffusion of the tumour cells.

Since  $IL_2$  diffuses through the tumour localization, and coupled with the elements already discussed in the previous paragraph, this leads to the PDE system

$$\frac{\partial E}{\partial t} = D_1 \nabla^2 E - \chi \nabla \cdot (E \nabla \alpha) + \rho R h(x) + \frac{\theta_1 E T}{g_1 + T} - d_1 E - l E T + \omega I L_2 R + \frac{\theta_2 E I L_2}{g_2 + I L_2} + c T, \quad (4.5a)$$

$$\frac{\partial T}{\partial t} = D_2 \nabla^2 T + a T (1 - b T) - m E T, \quad (4.5b)$$

$$\frac{d I L_2}{dt} = D_4 \nabla^2 I L_2 + s_2 + \frac{\theta_3 E T}{g_3 + T} - d_2 I L_2, \quad (4.5c)$$

$$\frac{\partial \alpha}{\partial t} = D_3 \nabla^2 \alpha + n E T - d_2 \alpha, \quad (4.5d)$$

$$\frac{\partial R}{\partial t} = D_5 \nabla^2 R + s_3 + a_2 R (1 - b_2 R) - \omega I L_2 R - \rho R, \quad (4.5e)$$

where  $D_4$  and  $D_5$  are the diffusion rates of  $IL_2$  and  $R$  respectively. We apply the zero flux boundary conditions to the  $IL_2$  and  $R$  and assume that their initial localization in the tissue is the same as that of the TICLs. In other words, the boundary and initial conditions for  $IL_2$  and  $R$  respectively are;

$$\frac{\partial I L_2}{\partial t}(0, t) = \frac{\partial R}{\partial t}(0, t) = 0, \quad (4.6)$$

$$I L_2(x, 0) = \begin{cases} 0 & \text{if } 0 \leq x \leq L \\ I L_{20} [1 - \exp(-1000(x - L)^2)] & \text{if } L \leq x \leq x_0. \end{cases} \quad (4.7)$$

$$R(x, 0) = \begin{cases} 0 & \text{if } 0 \leq x \leq L \\ R_0 [1 - \exp(-1000(x - L)^2)] & \text{if } L \leq x \leq x_0. \end{cases} \quad (4.8)$$

In our case  $L = 0.2$ , as assumed in Chapter 3. We non-dimensionalize system (4.5) as previously done by taking  $IL_2$  and  $R$  as a fractions of their initial densities.

Time is nondimensionalized with respect to immune cell diffusion, ie,

$$\bar{E} = \frac{E}{E_0}, \quad \bar{T} = \frac{T}{T_0}, \quad \bar{\alpha} = \frac{\alpha}{\alpha_0}, \quad I\bar{L}_2 = \frac{IL_2}{IL_{20}}, \quad \bar{R} = \frac{R}{R_0}, \quad \text{and} \quad \bar{t} = \frac{t}{t_0}.$$

The bars are dropped for convenience, to give the system of equations

$$\begin{aligned} \frac{\partial E}{\partial t} = & \nabla^2 E - \chi \nabla \cdot (E \nabla \alpha) + \bar{\phi}_1 R h(x) + \frac{\bar{\theta}_1 E T}{\eta_1 + T} - \psi E - \nu E T + \bar{\omega}_1 I L_2 R + \frac{\bar{\theta}_2 E I L_2}{\eta_2 + I L_2} \\ & + \bar{c} T, \end{aligned} \quad (4.9a)$$

$$\frac{\partial T}{\partial t} = \phi \nabla^2 T + \beta_1 T (1 - \beta_2 T) - \bar{\mu}_1 E T, \quad (4.9b)$$

$$\frac{d I L_2}{dt} = \zeta \nabla^2 I L_2 + \sigma_2 + \frac{\bar{\theta}_3 E T}{\eta_3 + T} - \bar{\mu}_2 I L_2, \quad (4.9c)$$

$$\frac{\partial \alpha}{\partial t} = \tau \nabla^2 \alpha + k E T - \delta \alpha, \quad (4.9d)$$

$$\frac{\partial R}{\partial t} = \zeta \nabla^2 R + \sigma_3 + \alpha_1 R (1 - \alpha_2 R) - \bar{\omega}_2 I L_2 R - \bar{\phi}_2 R, \quad (4.9e)$$

where

$$\begin{aligned} \lambda = \chi \alpha_0 t_0, \quad \bar{\theta}_1 = \theta_1 t_0, \quad \psi = d_1 t_0, \quad \bar{\theta}_2 = \theta_2 t_0, \quad \eta_2 = g_2 t_0, \\ \bar{\omega}_1 = \frac{\omega R_0 I L_{20} t_0}{E_0}, \quad \eta_1 = \frac{g}{T_0}, \quad \nu = l T_0 t_0, \quad \phi = D_2 t_0, \quad \beta_1 = a t_0, \\ \bar{\mu}_1 = m E_0 t_0, \quad \tau = D_3 t_0, \quad \kappa = \frac{n E_0 T_0 t_0}{\alpha_0}, \quad \delta = d_2 t_0, \quad \beta_2 = b T_0, \\ \zeta = D_4 t_0, \quad \bar{\theta}_3 = \theta_3 t_0, \quad \eta_3 = g_3 t_0, \quad \bar{c} = \frac{c T_0 t_0}{E_0}, \quad \sigma_3 = \frac{s_3 t_0}{R_0}, \end{aligned}$$

$$\bar{\phi}_1 = \frac{\rho R_0 t_0}{E_0}, \quad \sigma_2 = \frac{\sigma_2 t_0}{I L_{20}}, \quad \zeta = D_5 t_0, \quad \bar{\mu}_2 = \mu_2 t_0,$$

$$\bar{\omega}_2 = \omega_2 t_0, \quad \alpha_1 = a_2 t_0, \quad \alpha_2 = b_2 R_0, \quad \bar{\phi}_2 = \rho t_0.$$

The boundary and initial conditions are, respectively;

$$\frac{\partial E}{\partial x}(0, t) = \frac{\partial I L_2}{\partial x}(0, t) = \frac{\partial R}{\partial x}(0, t) = \frac{\partial T}{\partial x}(0, t) = \frac{\partial \alpha}{\partial x}(0, t) = 0,$$

$$\frac{\partial E}{\partial x}(1, t) = \frac{\partial R}{\partial x}(1, t) = \frac{\partial I L_2}{\partial x}(1, t) = \frac{\partial T}{\partial x}(1, t) = \frac{\partial \alpha}{\partial x}(1, t) = 0,$$

$$\begin{aligned}
 E(x,0) &= \begin{cases} 0, & 0 \leq x \leq L \\ [1 - \exp(-1000(x-L)^2)], & L \leq x \leq x_0, \end{cases} \\
 R(x,0) &= \begin{cases} 0, & 0 \leq x \leq L \\ [1 - \exp(-1000(x-L)^2)], & L \leq x \leq x_0, \end{cases} \\
 IL_2(x,0) &= \begin{cases} 0, & 0 \leq x \leq L \\ [1 - \exp(-1000(x-L)^2)], & L \leq x \leq x_0, \end{cases} \\
 T(x,0) &= \begin{cases} [1 - \exp(-1000(x-L)^2)], & 0 \leq x \leq L \\ 0, & L \leq x \leq x_0, \end{cases} \\
 \alpha(x,0) &= 0, \forall x \in [0, x_0].
 \end{aligned}$$

Using a similar method as in Chapter 3, Section 3.5, we discretize model (4.9) using the Crank Nicholson method. The tridiagonal matrices for the TICLs, tumour and chemokine concentrations remain the same. The right hand sides of the tumour and chemokine equations ( $b_T$  and  $b_\alpha$ ) also remain the same except for  $b_E$ . The tridiagonal matrices for  $IL_2$  and  $R$  equations are

$$A_{IL_2} = \begin{pmatrix} P_4 - W_4 & -W_4 & 0 & \cdots & \cdots & 0 \\ -W_4 & P_4 & -W_4 & 0 & 0 & \vdots \\ 0 & -W_4 & P_4 & -W_4 & 0 & \vdots \\ \vdots & \vdots & \vdots & \vdots & 0 & \\ \vdots & 0 & 0 & -W_4 & P_4 & -W_4 \\ 0 & 0 & 0 & 0 & -2W_4 & P_4 \end{pmatrix} \begin{pmatrix} IL_2_1^{j+1} \\ IL_2_2^{j+1} \\ \vdots \\ \vdots \\ IL_2_{N-1}^{j+1} \\ IL_2_N^{j+1} \end{pmatrix},$$

and

$$A_R = \begin{pmatrix} P_5 - W_5 & -W_5 & 0 & \cdots & \cdots & 0 \\ -W_5 & P_5 & -W_5 & 0 & 0 & \vdots \\ 0 & -W_5 & P_5 & -W_5 & 0 & \vdots \\ \vdots & \vdots & \vdots & \vdots & 0 & \\ \vdots & 0 & 0 & -W_5 & P_5 & -W_5 \\ 0 & 0 & 0 & 0 & -2W_5 & P_5 \end{pmatrix} \begin{pmatrix} R_1^{j+1} \\ R_2^{j+1} \\ \vdots \\ \vdots \\ R_{N-1}^{j+1} \\ R_N^{j+1} \end{pmatrix},$$

respectively where

$$W_4 = \frac{\xi}{2h^2}, \quad W_5 = \frac{\zeta}{2h^2}, \quad P_4 = \frac{2W_4 dt + 1}{dt}, \quad \text{and} \quad P_5 = \frac{2W_5 dt + 1}{dt}.$$

#### 4.6.2 Numerical solutions

We simulate the model using parameter values in Tables 2.3, 3.1, and 4.3. For these simulations, we also assumed that  $R$  and  $IL_2$  diffuse at the same rate as TICLs (ie  $D_1 = D_4 = D_5 = 10^{-6}$ ). We chose to simulate the model for a long time period (hundreds and thousands of days) because in reality, tumour formation and cancer progression takes a long time. Figure 4.4 gives the solutions for the tumour and TICLs cell densities against distance into the tissue after incorporating space and with immunotherapy. In Figures 4.4(a)-(d), we used *twinx* in *PYTHON* to set the TICLs and tumour cell densities on different scales, so as to compare the two. The right hand side corresponds to the tumour cell density while the left hand side corresponds to TICLs density. Comparing Figures 4.4(a)-(d) to Figures 3.2(a)-(d), we observe that the tumour cell density drops to more than half that in Figure 3.2. We also observe that the TICL density is increased through out the tissue and the tumour penetration in the tissue drops to half that of Figure 3.2. Finally, a lower tumour cell density is observed, going by the peaks of the graphs.

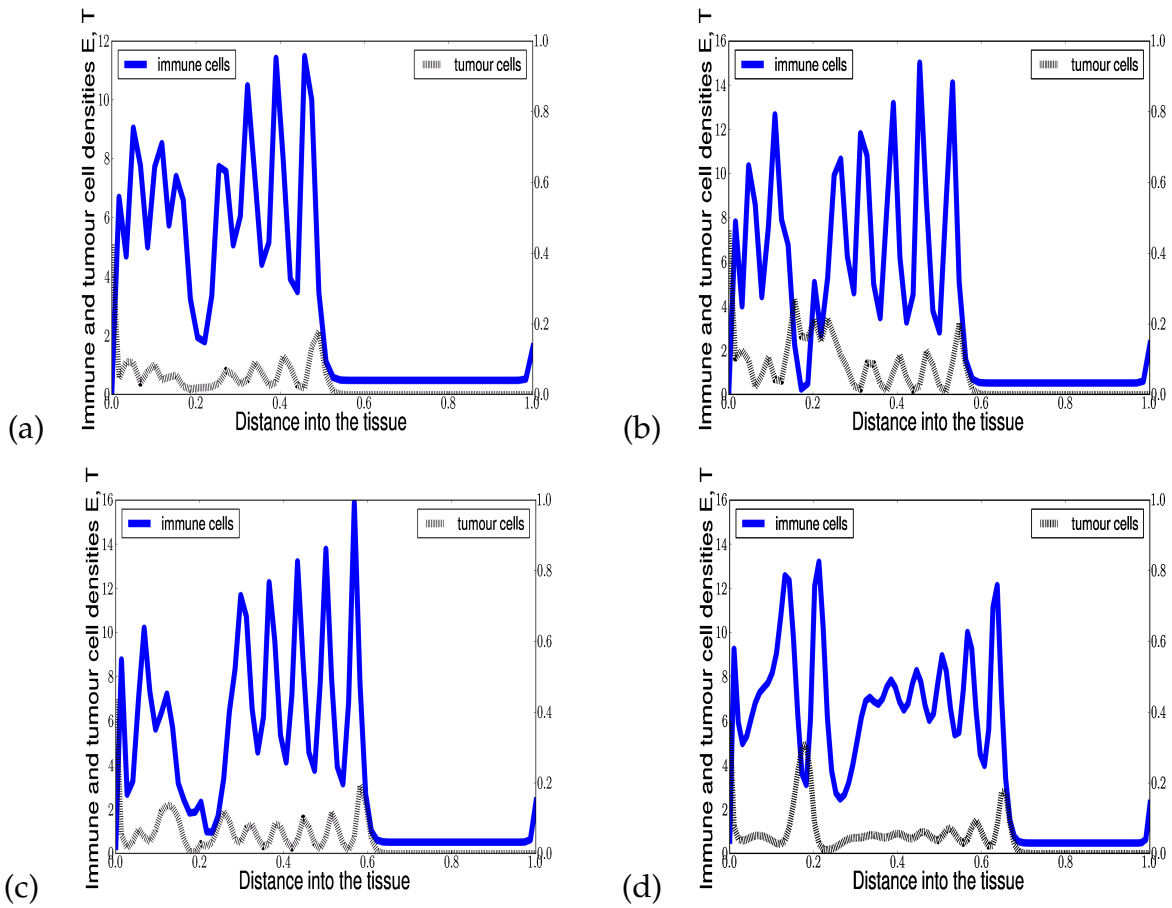


Figure 4.4: Plots of solutions showing spatial distribution of immune (TICLs) and tumour cell densities with immunotherapy in the tissue at times corresponding to (a) 600, (b) 700, (c) 800 and (d) 1000 days respectively. The left and right hand scales correspond to TICLs and tumour cell densities respectively.

In this Chapter we formulated a model that includes immunotherapy to investigate TICL-tumour interactions by extending the model of of Matzavinos et al. [6] and also introducing a new class of resting TICLS. We determined the steady state solutions to predict the long term behaviour of the system (4.4). We analysed the model's phase space and determined numerical solutions. We showed that while  $IL_2$  did not enhance the effectiveness of TICLS to completely eradicate the tumour cells, it aided in quickly converging the solutions to a cancer dormant state. Like in Chapter 3, we considered diffusion of TICLS,  $IL_2$ , and tumour cells and chemotaxis of TICLS to incorporate spatial distribution of cells. We used the Crank Nicholson method to numerically solve the resulting system of equations (4.9). The numerical solutions suggested that tumour cell density drops to more than half that in 4.4. We also observe that the TICL density is increased throughout the tissue. These results suggest that immunotherapy enhances the probability of TICLS eradicating the tumour cells but still do not completely eliminate them from the tissue. Immunotherapy helps to achieve cancer dormancy (the state to which the TICLS and tumour cells converge).

# Chapter 5

## Conclusion

The objective of this study was to examine the interaction between immune cells particularly TICLs and tumour cells and to investigate the phenomenon of cancer dormancy as a result of these cell interactions using mathematical models. In doing so, we determined the homogeneous models' equilibria and investigated their stability, we found a threshold for the homogeneous model without treatment and established a condition for the existence of a stable tumour free equilibrium state. We analysed the phase spaces by determining the most important parameter values that need to be targeted to eradicate cancer in body tissue. We investigated the existence of periodic solutions and plotted the phase portraits of the models. For the heterogeneous model without treatment, we investigated the existence of travelling wave solutions in the phase space. Numerical simulations were compared to analytical predictions, where possible.

In Chapter 2 we considered a 5D TICL-tumour interaction model by Matzavinos et al. [6] and reduced it to a 2D model by making two major assumptions:

- the formation of cellular conjugates occurs on a time scale of a few hours while that of tumour cells as well as the influx of immune cells into the

spleen occurs on a much slower time scale, probably tens of hours

(i.e.  $\frac{dC}{dt} \approx 0$ ).

- the dead immune and tumour cells do not influence the formation of cellular conjugates.

We analysed the 2D model to determine the nature of interaction of TICLs and tumour cells. The model gave one healthy steady state that was unstable and one cancer dormant state that was stable. Some studies such as Wordaz and Jansen [41], have shown that a tumour may disappear but after some time regrow to a lethal size. In our analysis, however, we do not achieve such a result. Our study showed that the TICLs brought the tumour cells to a cancer dormant state but did not completely eliminate them from the tissue. We determined a threshold condition,  $R_0$ , for the healthy steady state (TFE) and showed that this is locally asymptotically stable for  $R_0 < 1$ . We used the centre manifold theory to prove that this healthy steady state is globally unstable. Sensitivity analysis showed that the tumour cell death parameter value is the most sensitive in influencing the phase space of the 2D system. We also showed that the 2D model does not exhibit a limit cycle, contrary to the results of Matzavinos et al. [6].

In Chapter 3 we incorporated space into our first model to account for the diffusion of TICLS and tumour cells in the tissue, and the movement by chemotaxis of the TICLs into the tissue. We used finite differences for this spatial distribution model and the Crank Nicholson method, because it is unconditionally stable. The model consisted of non-linear coupled PDEs and the non-linearities are evaluated at the  $j$ th level, where the node values are known. The simulations showed oscillations of densities of both TICLs and tumour cells inside the tissue and less tumour cells outside the tissue. We carried out travelling wave analysis and showed that our model exhibited travelling wave solutions. The existence of travelling wave

solutions confirmed the expectation that the density of the TICLs would outweigh that of the tumour cells in the tissue. However, in reality, it may not be the case.

In Chapter 4 we developed two new models which incorporated immunotherapy, one described local interaction kinetics of TICLs-tumour cell interaction and the other incorporating space. In developing these models, we introduced a new class of cell concentration, that is the resting TICLs, the cells from which hunting TICLs are recruited. Our choice of immunotherapy over other cancer interventions was motivated by the particular models we had developed in Chapters 2 and 3. Other interventions, such as chemotherapy, radiotherapy and surgery would completely change the structure of the first two models and so were not part of this study. Our analysis of both the homogeneous and the spatial temporal models revealed that immunotherapy aids TICLs in bringing the tumour density to a lower level but does not completely eradicate cancer in the tissue. The spatial distribution of the TICLs and tumour cell densities, in the second model with immunotherapy, remained almost the same as before (without immunotherapy) although the tumour cell concentration in the tissue was lowered. In future, we will further extend these models by considering mixed cancer intervention methods, possibly chemotherapy and immunotherapy or radiotherapy and immunotherapy or radiotherapy and chemotherapy. The investigations would focus on the TICLs-tumour interactions, and the efficacy of each of these treatments. We hope to further extend the study to consider diffusion and chemotaxis in higher dimensions to give more accurate insights into TICLs-tumour interactions because in reality, the geometry of human body tissue is very complex.

# Appendix 1- Glossary

- **Apoptosis** (pages 10, & 11)- is a process of programmed cell death that may occur in multicellular organisms.
- **Avascular** (pages 3, 4, 7, 9, 10, 16, 24 & 45 )- is a stage in cancer growth where a tumour nodule is not supplied with any sort of nutrients by blood vessels.
- **Chemokine** (pages 5, 13, 14, 17, 23, 43, 47, & 79) - is a cytokine, or signalling protein type secreted by cells.
- **Chemotaxis** (pages i, 5, 7, 8, 10, 11, 12, 14, 15,18, 19, 20, 44, 45, 48, 50, 53, 57, 58, 77, 82, & 84) - is the phenomenon whereby tumour and immune cells direct their movements according to certain chemicals in their environment.
- **Kinetics** (pages 12, 13, 19, 23, 44, 46, 62, & 85)- is a rate of change in a Biochemical reaction.
- **Mitosis** (10, 16, & 46)- is a stage in cell cycle formation.
- **Nascent cells** (page 4)- are cells that are just coming into existence and beginning to display signs of future potential.
- **Necrotic core** (page 4)- Is a layer in a tumour nodule that contains cells that are dead.
- **Proliferating cells** (page 4)- is a layer in a tumour nodule containing cells that are reproducing or replicating.
- **Quiescent layer** (page 4)- is a layer in a tumour nodule that lies between the proliferating layer and the necrotic core.
- **Somatic cells** (5, 45) - is any biological cell forming the body of an organism.
- **Tumour nodule** (pages 4, 5, 27, & 44) is a relatively hard solid that is formed by an abnormal growth of neoplastic cells. It can be cancerous (malignant) or non-cancerous (benign).

## Appendix 2- List of Abbreviations

**BCL<sub>1</sub>** Marine B-cell Lymphoma.

**CD8<sup>+</sup>** Cluster of Differentiation 8.

**CT** Computed Tomography.

**DCs** Dendritic cells.

**DTI** Diffusion Tensor Images.

**GVAX** Cell Genesys.

**IL2** Interleukine-2.

**IMR** Magnetic Resonance Images.

**IFN<sub>γ</sub>** Interferon-gamma.

**LAK** Lymphokine Activated Killer Cells.

**NK** Natural Killer Cells.

**TAF** Tumour Angiogenetic Factors.

**TICLs** Tumour Infiltrating Cytotoxic Lymphocytes (same as Cytotoxic T-lymphocytes, **CTLs**)

## Appendix 3- List of parameters

Parameter	Description
$k_1$	Rate of binding of TICLs to tumour cells.
$k_{-1}$	Rate of detachment of TICLs from tumour cells without damaging the cells.
$k_2$	Rate of detachment of TICLs from tumour cells resulting into cell death.
$p$	Probability of de-activating/killing tumour cells.
$k_2p$	Death rate of tumour cells.
$k_2(1 - p)$	Death rate of TICLs.
$s$	Rate of normal flow of mature TICLs into the tumour localisation.
$d_1$	Natural death rate of TICLs.
$d_2$	Rate of decay of de-activated TICLs.
$d_3$	Rate of decay of lethally hit/dead tumour cells.
$a$	Intrinsic tumour growth rate.
$1/b$	Tumor carrying capacity.
$D_1$	TICLs diffusion coefficient.
$D_2$	Tumour diffusion coefficient.
$D_3$	Chemokine diffusion coefficient.
$k_3$	Chemokine production rate.
$\chi$	Chemotaxis coefficient.
$d_4$	Deactivation rate of the chemokine concentration.
$s_2$	Rate of $IL_2$ is supply (amount of $IL_2$ injected into the tissue).
$s_3$	Rate of resting cells supply.
$\omega$	Stimulation rate of resting cells to hunting cells as a result of $IL_2$ supply.
$\rho$	Recruitment rate of TICLs from the resting cells.
$c$	Ability of $IL_2$ to provoke an immune response (antigenicity rate).
$a_2$	Growth rate of resting cells.
$b_2$	inverse of carrying capacity for resting cells.
$d_2$	Rate of decay of $IL_2$ .

# References

- [1] American Cancer Society. (2013) *The history of cancer*. Available from <http://www.cancer.org/>, accessed on 11.05.2013.
- [2] MedicineNet.com. (2011) *Definition of a tumour*. Available from <http://www.medterms.com/script/main/art.asp?articlekey=5863>, accessed on 01.03.1013.
- [3] M. M. Melicow. (1982) The new steps to cancer. *J. Theoretical Biology*, **94**, 471-511.
- [4] M. Yashiro, J. M. Carethers, L. Laghi, K. Saito, P. Slezak, E. Jaramillo, C. Rubio, K. Koizumi, K. Hirakawa, and C.R. Boland. (2001) Genetic pathways in the evolution of morphologically distinct colorectal neoplasms. *J. Cancer Research*, **61**, 2676-2683.
- [5] World Health Organization. (2012) *Cancer report*. Available from <http://www.who.int/cancer/en/>, accessed on 11.05.2013.
- [6] A. Matzavinos, M. A. J. Chaplain, and V. A. Kuznetsov. (2004) Mathematical modelling of spatio-temporal response of cytotoxic T-lymphocytes to a solid tumour. *J. Mathematical Medicine and Biology*, **21**, 1-34.
- [7] A. Zeyton, M. Hassuneh, M. Nagarkatti, and P. S. Nagarkatti. (1997) Fas-Fas ligand-based interactions between tumour cells and tumor-specific cytotoxic

- T lymphocytes; A lethal two-way Street. *J. American Society of Hematology*, **90**, 1952-1959.
- [8] R. M. Sutherland. (1988) Cell and environmental interactions in tumour microregions: The multicell spheroid model. *J. Science*, **240**, 177-184.
- [9] M. A. J. Chaplain. (1996) Avascular growth, angiogenesis and vascular growth in solid tumors: The mathematical modelling of the stages of tumour development. *J. Computational Modelling*, **23**, 47-87.
- [10] J. A. Aguirre-Gisho. (2007) Models, mechanisms and clinical evidence for cancer dormancy. *J. Cancer*, **7**, 834-846.
- [11] B. Perthame. (2004) PDE models for chemotactic movements: parabolic, hyperbolic and kinetic. *J. Applications of Mathematics*, **6**, 539-564.
- [12] R. A. Deweger, B. Wilbrink, R.M.P. Moberts, D. Omans, R. Oskam, and W Den Oten. (1987) Immune reactivity in SL2 lymphoma-bearing mice compared with SL2-immunized mice. *J. Immunotherapy*, **24**, 1191-1192.
- [13] P. L. Lollini, A. Palladini, F. Pappalardo, and S. Motta. (2008) Predictive models in tumour immunology in *Selected topics on cancer modelling: genesis, evolution, immune competition and therapy*, N. Bellomo, M. Chaplain, and E. De Angelis (Eds). Birkhauser, Boston, 363-384.
- [14] M. J. Smyth, G. P. Dunn, and R. D. Schreiber. (2006) Cancer immunosurveillance and immunoediting: the roles of immunity in suppressing tumour development and shaping tumour immunogenicity. *J. Immunology*, **90**, 1-50.
- [15] S. A Rosenberg, J. C. Yang, and N. P. Restifo. (2004) Cancer immunotherapy: moving beyond current vaccines. *J. Medicine*, **10**, 909-915.

- 
- [16] A. E Radunskaya, L.G. de Pillis, and W. Gu. (2006) An analysis of mixed immunotherapy and chemotherapy. *J. Theoretical Biology*, **4**, 841-62.
- [17] T. A. Hadji. (2005) Alemtuzumab for B-cell chronic lymphocytic leukemia. *J. Health Technology*, **66**, 1-4.
- [18] J. Li, K. Guo, V. W. Koh, J. P. Tang, BQ. Gan, H. X. Li, and Q. Zeng. (2005) Generation of PRL-3 and PRL-1 monoclonal antibodies as potential diagnostic makers for cancer metastases. *J. Clinical Cancer*, **11**, 2195-2204.
- [19] chemoth.com. (2013) *Tumour growth models*. Available from <http://chemoth.com/tumorgrowth>, accessed on 01.03.2013.
- [20] A. K. Laird. (1964) Dynamics of tumour growth. *J. Cancer*, **18**, 490-502.
- [21] P. Breuer, W. Huber, and F. Petruccione. (1993) Fluctuation effects on wave propagation in a reaction-diffusion process. *Physica D: Nonlinear Phenomena*, **73**, 259-273.
- [22] T. Rose, S. J Chapman, and P. K. Maini. (2007) Mathematical models of avascular tumour growth. *J. Industrial and Applied Mathematics*, **49**, 179-208.
- [23] J. Murray (2002) *Mathematical Biology*. Springer-Verlag, New York.
- [24] health-e-child.org. (2004) *Tumour growth modelling in the brain*. Available from [http://www-sop.inria.fr/asclepios/projects/Health-e-Child/DiseaseModels/content/brain/TumorGrowth1\\_review.html](http://www-sop.inria.fr/asclepios/projects/Health-e-Child/DiseaseModels/content/brain/TumorGrowth1_review.html), accessed on 27.03.2013.
- [25] R. Araujo, and D. McElwain. (2004) A history of the study of solid tumour growth: the contribution of mathematical modelling. *J. Mathematical Biology*, **66**, 111-187.

- 
- [26] A. Boondirek, Y. Lenbury, J. Wong-ekkabut, W. Triampo, I. M. Tang, and P. Picha. (2006) A Stochastic Model of Cancer Growth with Immune Response. *J. Theoretical Biology*, **49**, 1652-1666.
- [27] A. S. Qi, X. Zheng, C.Y. Du, and B. S. (1993) A cellular automation of cancerous growth. *J. Theoretical Biology*, **161**, 1-12.
- [28] E. A. Reis , L. B. L. Santos, and S. T. R. Pinho. (2009) A cellular automata model for avascular solid tumour growth under the effect of therapy. *J. Physica A*, **388**, 1303-1314.
- [29] J. Smolle, and H. Stettner. (1993) Computer simulation of tumour cell invasion by a stochastic growth model. *J. Theoretical Biology*, **160**, 63-72.
- [30] P. B. Ashwin, M.V. Bartucelli, T. J. Bridges, and S.A. Gourley. (2002) Traveling fronts for the KPP equation with spatio-temporal delay. *J. Maths. Physics*, **53**, 103-122.
- [31] J. Jaaskelainen, A. Maenpaa, A. Patoproyo, M. Gahmberg, C. G. Somersalo, K. Tarkkanen, J. Kallio, and T. Timonen. (1992) Migration of recombinant IL-2-activated T-cells and natural killer cells in the inter cellular space of human H-2 glioma spheroids in vitro-a study of adhesion molecules involved instabilities. *J. Immunology*, **149**, 260-268.
- [32] D. Kirschener, and J.C. Panetta. (1998) Modelling immuotherapy of the tumour immune interaction. *J. Mathematical Biology*, **37**, 235-252.
- [33] E. Konukoglu, O. Clatz, B.H. Menze, B. Stieltjes, M. Weber, E. Mandonnet, H. Delingette, and N. Ayache. (2010) Image guided personalization of reaction-diffusion type tumour growth models using modified anisotropic Eikonal equations. *J. Medical Imaging*, **29**, 78-95.

- 
- [34] K. Swanson, E. Alvord, and J. Murray. (2002) Virtual brain tumours (gliomas) enhance the reality of medical imaging and highlight inadequacies of current therapy. *J. Cancer*, **86**, 14-18.
- [35] G. Cruywagen, D. Woodward, P. Tracqui, G. Bartoo, J. Murray, and E. Alvord. (1995) The modelling of diffusive tumours. *J. Biological Systems*, **3**, 937-945.
- [36] M. R. Myerscough, P.K. Maini, J. D. Murray, and K. H. Winters. (1998) Two dimensional pattern formation in a Chemotactic model. *J. Mathematical Biology*, **60**, 1-26.
- [37] V. Hornark, R. Dvorsk, and E. Sturdik. (1999) Receptor-Ligand interaction and molecular modelling. *J. Biophysics*, **18**, 231-248.
- [38] D. A. Lauffenburger, and J. J. Linderman. (1993) *Models for binding, trafficking, and signalling*. New York: Oxford University Press.
- [39] P. M. Dean. (1987) *Molecular foundations of drug-receptor interaction*. Cambridge University Press, Cambridge.
- [40] Y. Kawakami, M. Nishimura, M. I. Restifo, N. P. Topalian, S.L. Oneil, and B. H. Shilyansky. (1993) T-cell recognition of human melanoma antigens. *J. Immunotherapy*, **14**, 88-93.
- [41] D. Wordaz, and A. A. Jansen.(2003) A dynamical perspective of CTL cross-priming and regulation:implications for cancer immunology. *J. Immunology*, **86**, 213-227.
- [42] S. P. Ellner, and J. Guckenheimer. (2006) *Dynamics models in Biology*. Princeton University Press, Priceton.

- 
- [43] A. Diefenbach, E. R. Jensen, A. M. Jamieson, and D. Raulet.(2001) Real and H60 Ligands of the NKG2D receptor stimulate tumour immunity. *J. Nature*, **413**, 165-171.
- [44] A. Bru', S. Albertos, J. Subiza, J. Lopez, G. Asenjo, and I. Bru'. (2003) The universal dynamics of tumour growth. *J. Biophysics*, **85**, 2948-2961.
- [45] Y. Kawarada, R. Ganss, N. Garbi, B. Sacher, T. and Arnold, and G. Hammerling. (2001) NK and CD8+T cell-mediate eradication of established tumours by peritumoral injection of CpG-containing oligodeoxynucleotides. *J. Immunology*, **161**, 5253-2001.
- [46] V. A. Kuznetsov, I. A. Makalkin, M. A. Taylor, and A. S. Pereson.(1994) Non-linear dynamics of immunogenic tumours: Parameter estimation and global bifurcation analysis *Bulletin of Mathematical Biology*, **56**, 295-321.
- [47] A. G. Dalglish, and M. Browning. (1996) *Tumour immunology*. Press Syndicate, University of Cambridge, London.
- [48] M. Bar-Eli. (1999) Role of interleukine-8 in tumor growth and metastasis of human melanoma. *J. Pathobiology*, **67**, 12-18.
- [49] N. F. Briton. (2003) *Essential mathematical biology*. Springer verlag. University of Bath.
- [50] Z. Fishelson, and G. Berke. (1997) Tumour cell destruction by cytotoxic T lymphocytes: The basis of of reduced antitumor cell activity in syngenic hosts. *J. Immunology*, **125**, 2018-2052.
- [51] V. A. Kuznetsov. (1981) A model for cytotoxic cellular immune process and its experimental application. *J.Applied Problems in the Theory of Dynamical Systems*, **4**, 14-43.

- 
- [52] V. Y. Bohman. (1976) *Metastasis of corpus uterus cancer*. Leningrad: Medicine, London.
- [53] P. van den Driache, and J. Watmough. (2005) Reproduction numbers and sub-threshold endemic equilibria for compartmental models of disease transmission. *J. Mathematical Biology*, **8**, 1-15.
- [54] C. Castillo-Chavez, Z. Feng, and W. Huang. (2002) On the computation of the basic reproduction ratio and its role on global stability. *J. Mathematical Biology*, **1**, 229.
- [55] S. Wiggins. (1990) *Introduction to non-linear dynamical systems and chaos*. Springer-Verlag, New york.
- [56] H. Siue, E.S. Vietta, R. D. May, and J. W. Uhr. (1986) Tumour dormancy; Regression of the BCL tumor and induction of a dormant tumour state in mice chimeric at the major histocompatibility complex. *J. Immunology*, **137**, 1376-1382.
- [57] J. W. Uhr, and R. Marches. (2011) Dormancy in a model of murine B cell lymphoma. *Cancer Biology*, **11**, 277-286.
- [58] A. H. Kyle, C. T. Chan, and A. I Michinton. (1999) Characterization of three-dimensional tissue cultures using electrical impedance spectroscopy. *J. Biophysics*, **76**, 2640-2648.
- [59] S. Sozzani, W. Luini, M. Molino, P. Jilek, B. Bottazi, and C. Cerletti. (1991) The signal transduction pathway involved in migration induced by a monocyte chemotactic cytokine. *J. Immunology*, **147**, 2215-2221.
- [60] C. M. Chairns, J. R. Gordon, F. Li, M. E. Baca-Estrada, T. Moyana, and J. Xiang. (2001) Lymphotaktin expression by engineered myeloma cells drives

- tumour regression: mediation by CD4+ and CD8+ T cells and neutrophils expressing XCR1 receptor. *J. Immunology*, **167**, 57-65.
- [61] H. Nomiyama, K. Hieshima, T. Nakayama, T. Sakaguchi, R. Fujisawa, S. Tanase, H. Nishiura, K. Matsuno, H. Takamori, Y. Tabira, T. Yamamoto, R. Muira, and O. Yoshie. (2001) Human CC chemokine liver expressed chemokine/CCL116 is a fractional for CCR1, CCR2, and CCR5, and constitutively expressed by hepatocytes. *J. Immunology*, **13**, 1021-1029.
- [62] N. Bellomo, M. Chaplain, and E. De Angelis. (2000) *Selected topics in cancer modelling*. Birkhauser.
- [63] J. Crank, and P. Nicolson. (2004) A practical method for numerical evaluation of solutions of partial differential equations of the heat conduction type. *Proceedings of the Cambridge Philosophical Society*, **43**, 50-67.
- [64] A. Matzavinos, and M. A. J Chaplain. (2004) Traveling-wave analysis of a model of the immune response to cancer. *J. Biologies*, **327**, 995-1008.
- [65] R. Sarkar, and S. Banerjee. (2005) Cancer self remission and tumour stability- a stochastic approach. *J. Mathematical Biosciences*, **196**, 65-81.
- [66] F. S. Borges, K.C. Iarosz, H. P. Ren, A. M. Batista, M. S. Baptista, R.L. Viana, S.R. Lopez, and C. Grebogi. (2013) Model for tumour growth with treatment by continuous or pulsed chemotherapy. *J. BioSystems*, 1-6.
- [67] E. Tritarelli, E. Rocca, U. Tests, G. Boccoli, A. Camagna, F. Calabresi, and C. Peschle. (1991) Adoptive immunotherapy with high-dose interleukin-2: kinetics of circulating progenitors correlate with interleukin-6, granulocyte colony-stimulating factor level. *J. Blood*, **77**, 741-749.

- [68] L. H. Cornelissen, D. Bronneberg, D. L. Bader, F. P. T. Baaijens, and C.W.J. Oomens. (2009) The transport profile of cytokines in epidermal equivalents subjected to mechanical loading. *J. Biomedical Engineering*, **37**, 1007-1018.